Hyperspectral Unmixing: Insights and Beyond

Wing-Kin (Ken) Ma

Department of Electronic Engineering, The Chinese University of Hong Kong

A Talk at School of Electrical and Computer Engineering,
National Technical University of Athens,
June 15, 2023

Acknowledgment

José Bioucas-Dias
IST, Portugal

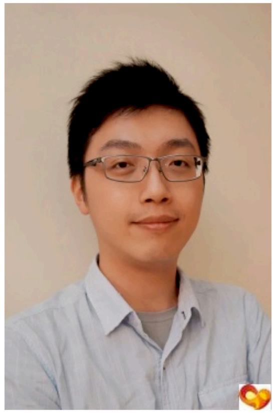

Tsung-Han Chan
MediaTek, Taiwan

Chong-Yung Chi
NTHU, Taiwan

Xiao Fu
Oregon State Univ., US

Nicolas Gillis
Univ. Mons, Belgium

Chia-Hsiang Lin
NCKU, Taiwan

Ruiyuan Wu
Meituan, Beijing

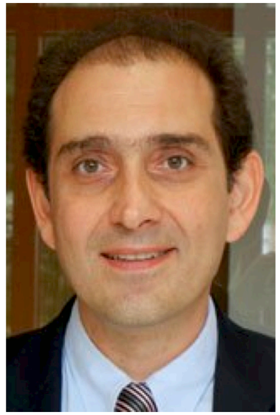

Nikos Sidiropoulos
Univ. Virgina, US

Background

Hyperspectral Imaging

- cover visible to near-infrared wavelengths, with 10nm resolution and > 200 bands

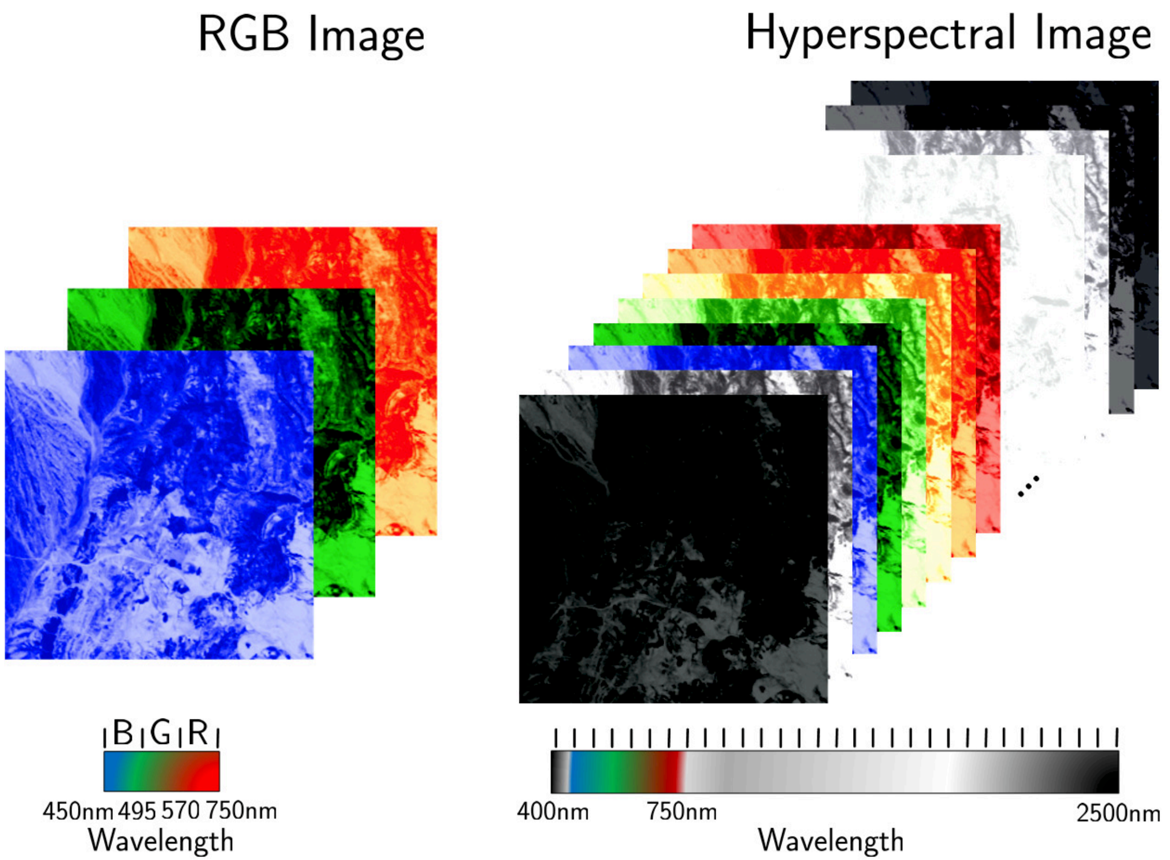

A Hyperspectral Image Example: Real or Fake?

A hyperspectral image shown in RGB. Captured by SPCIM IQ HS camera.

A Hyperspectral Image Example: Real or Fake?

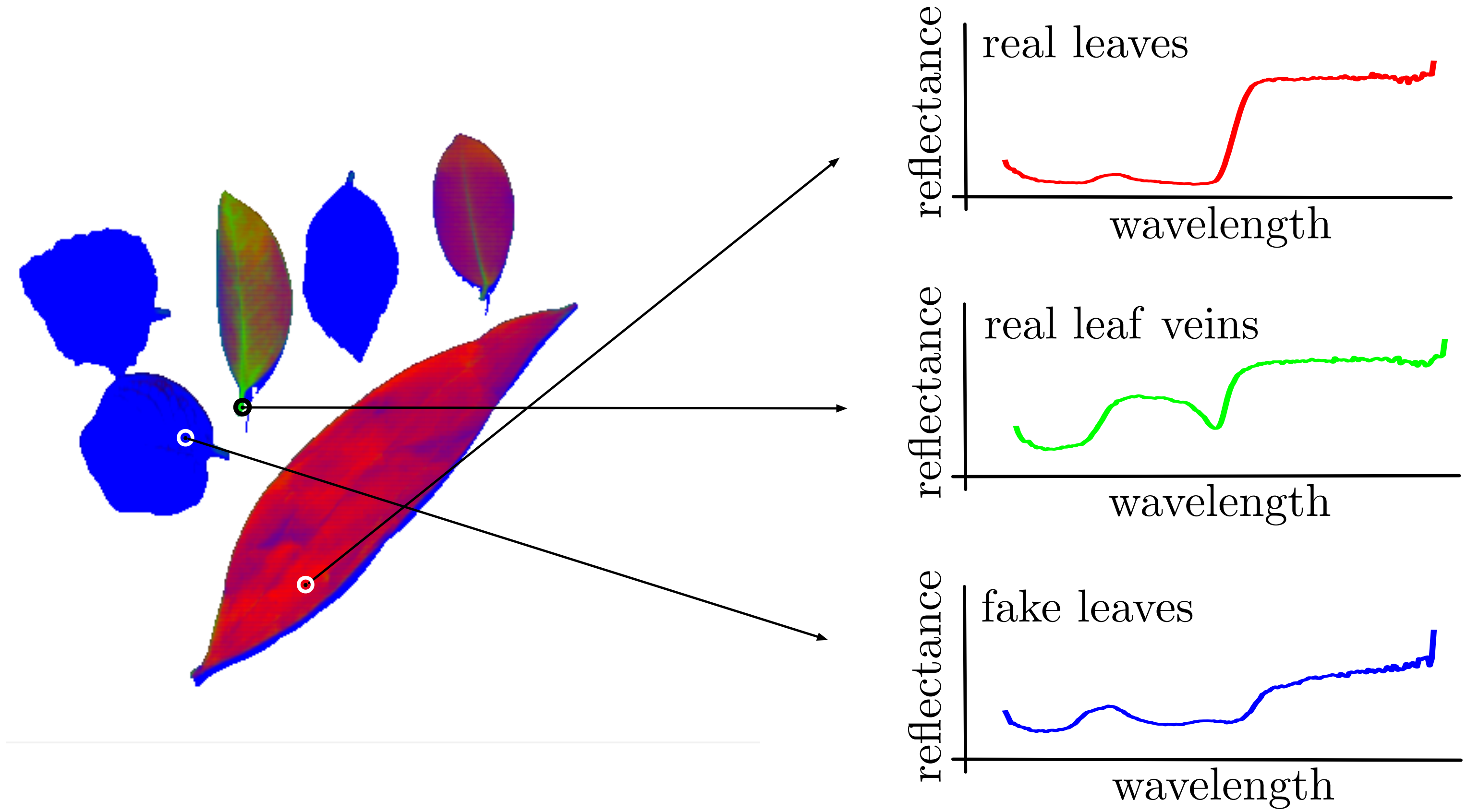

A false colormap of its underlying materials. Taking out the background, the image is composed of real leaves, leaf veins, and fake leaves.

Why Hyperspectral?

- allow us to “see” different materials, revealed by their spectral signatures

Example: Mineral Identification in Remote Sensing

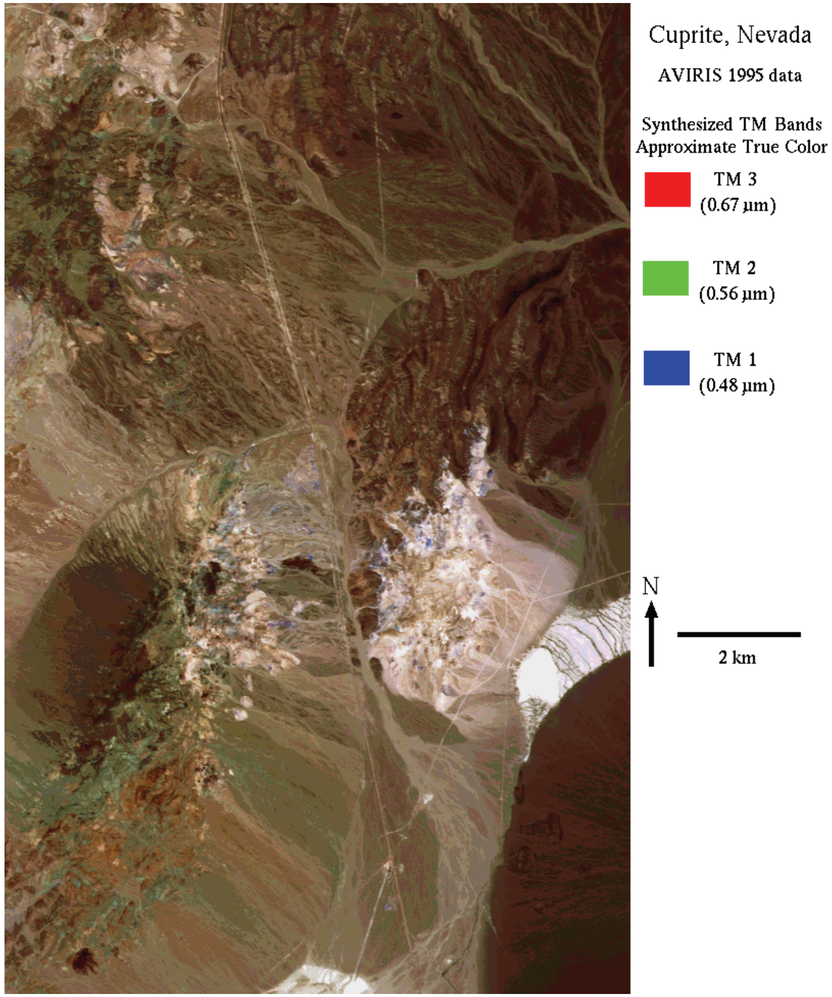

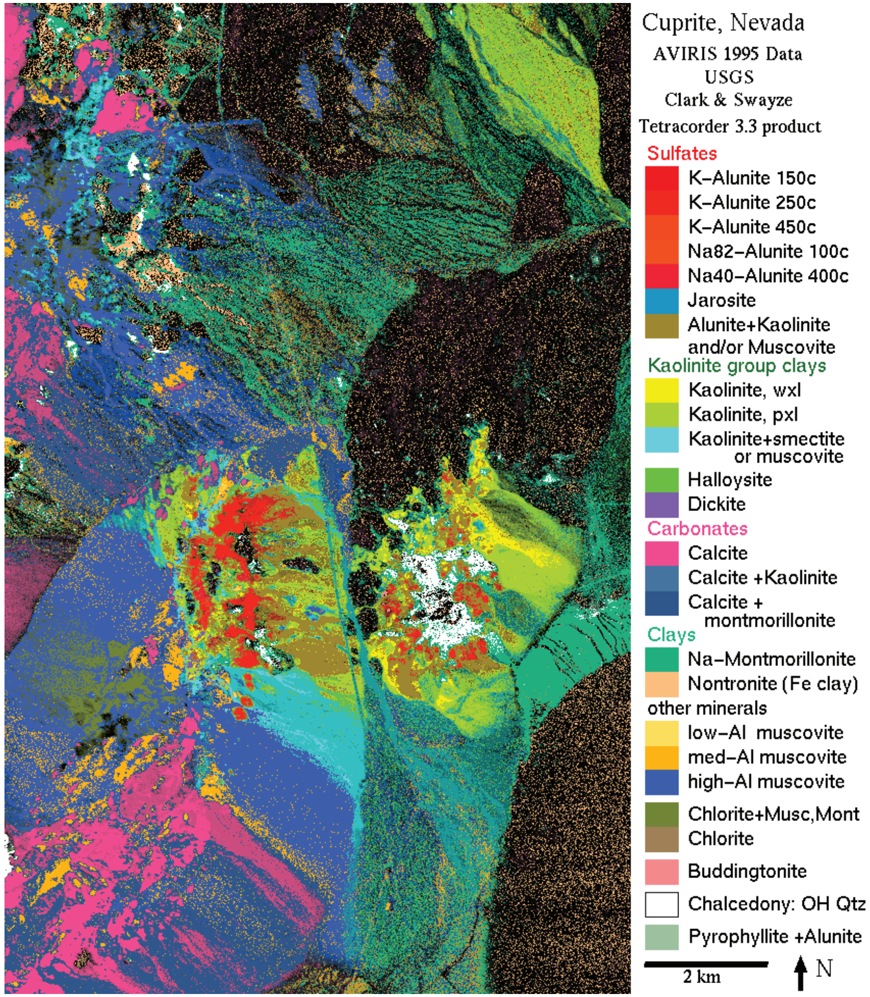

AVIRIS Cuprite image. Courtesy to USGS.

Applications

- remote sensing (studied extensively)
- food safety, art conservation, archaeology, medical imagery,...

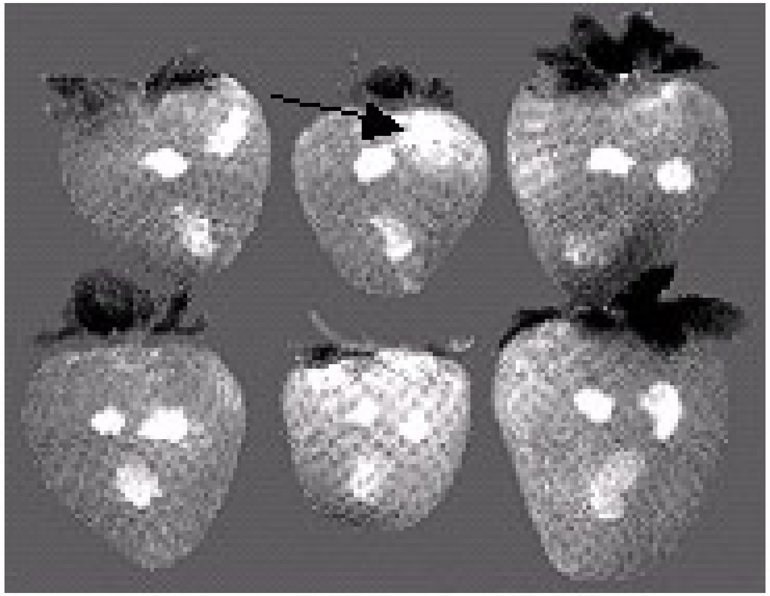

(a) food safety

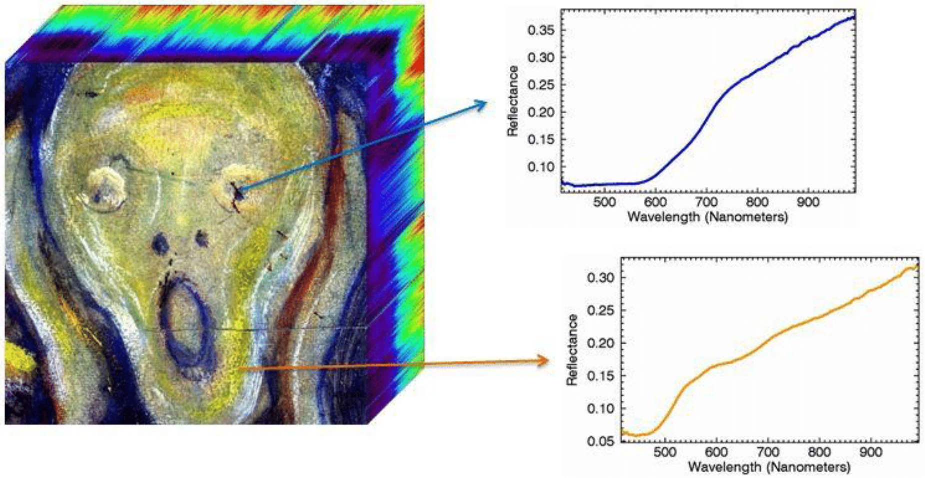

(b) pigment identification in art conservation

Source: (a) http://tao.umd.edu/html/fecal_contamination.html (b) H. Deborah, Pigment Mapping of Cultural Heritage Paintings Based on Hyperspectral Imaging, MSc Thesis, Gjøvik University College, Norway.

What We Will See in This Talk

- hyperspectral unmixing (HU), a key topic in remote sensing with nearly 30 years of history

- a study of an essentially simplex-structured matrix factorization problem:

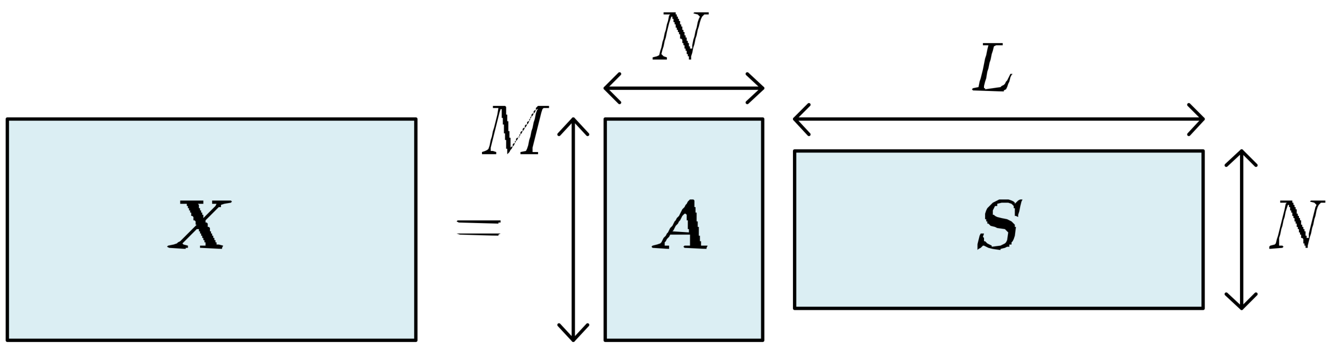

  where

  - $\boldsymbol{A}$ has full column rank;
  - every column of $\boldsymbol{S}$ lies in the unit simplex, i.e., $\boldsymbol{s}_i \geq \boldsymbol{0}, \boldsymbol{s}_i^T \boldsymbol{1} = 1$ for all i

- a branch of structured matrix factorization methods that has identifiability guarantees in theory

What Do You Mean by Identifiability Guarantees?

- for example, consider non-negative matrix factorization (NMF)

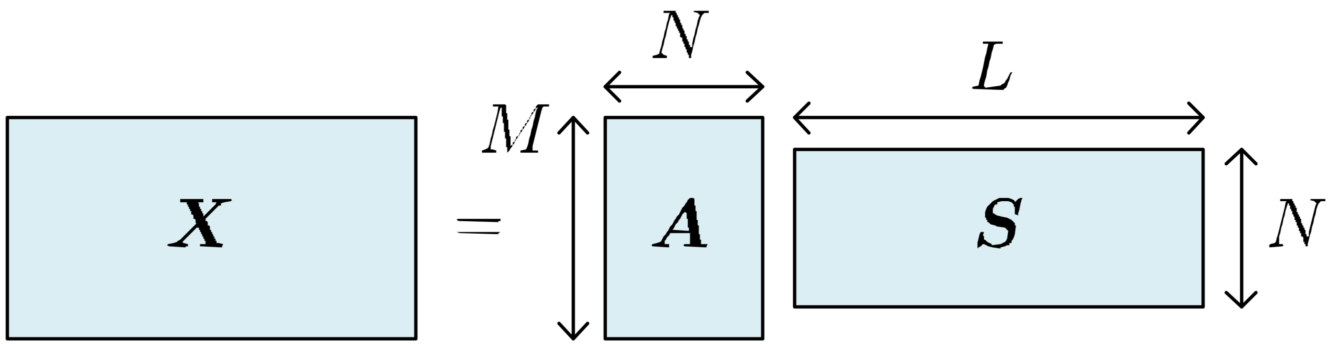

where $\boldsymbol{A} \geq \mathbf{0}, \boldsymbol{S} \geq \mathbf{0}$

- we want the true $(\boldsymbol{A}, \boldsymbol{S})$ to be recoverable (subject to trivial effects)

- observe

$$\boldsymbol{X} = \boldsymbol{A}\boldsymbol{S} = \underbrace{\boldsymbol{A}\boldsymbol{C}}_{=\tilde{\boldsymbol{A}}} \underbrace{\mathrm{C}^{-1}\boldsymbol{S}}_{=\tilde{\boldsymbol{S}}}, \qquad \text{for some invertible } \boldsymbol{C}$$

If $\tilde{\boldsymbol{A}}, \tilde{\boldsymbol{S}} \geq \mathbf{0}$, then $(\tilde{\boldsymbol{A}}, \tilde{\boldsymbol{S}})$ is also an NMF solution; NMF may not recover $(\boldsymbol{A}, \boldsymbol{S})$

Outline of this Talk

- HU model, the notion of convex geometry
- pure-pixel search, or separable NMF
- applications beyond HU
- (highlight) simplex volume minimization
- if time permits, probabilistic simplex component analysis and hyperspectral super-resolution
- HU is a rich topic. We will not go through Bayesian methods (via Monte Carlo), dictionary-aided sparse regression, simplex volume maximization, minimum volume enclosing ellipsoid, maximum volume inscribed ellipsoid, nonlinear unmixing, endmember variability,...

HU: Linear Spectral Mixture Model

- **Postulate:** a pixel is a linear proportional combination of pure materials
- example:

  a hyperspectral pixel (as reflectance) $= X\%$ spectral signature of water$+$
  $Y\%$ spectral signature of soil $+ Z\%$ spectral signature of vegetation

where $X\% + Y\% + Z\% = 100\%$.

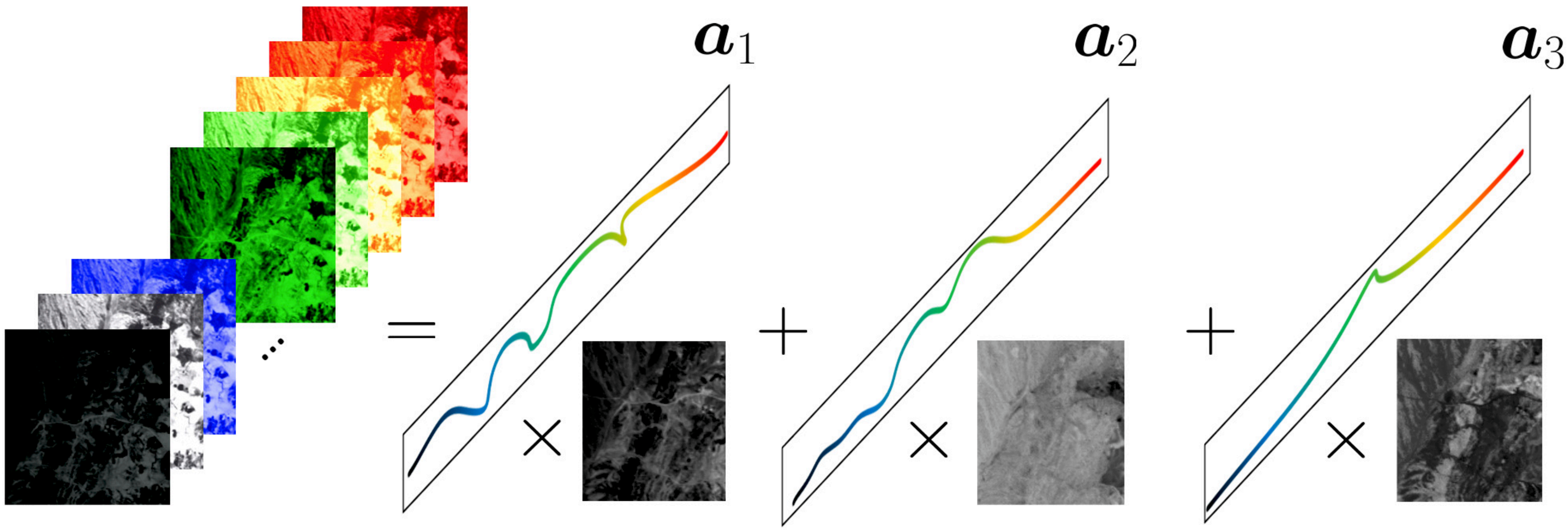

HU: Linear Spectral Mixture Model

- **Model:**

$$\boldsymbol{y}[n] = \sum_{i=1}^{N} \boldsymbol{a}_i s_i[n] + \boldsymbol{\nu}[n] = \boldsymbol{A}\boldsymbol{s}[n] + \boldsymbol{\nu}[n], \quad n = 1, \ldots, L,$$

where
  - $\boldsymbol{y}[n] \in \mathbb{R}^M$ is the measured hyperspectral vector at pixel n;
  - $\boldsymbol{A} = [\boldsymbol{a}_1, \ldots, \boldsymbol{a}_N]$, $\boldsymbol{a}_i \in \mathbb{R}^M$ is an endmember signature vector;
  - $\boldsymbol{s}[n] \in \mathbb{R}^N$ is the abundance vector at pixel n, with $\boldsymbol{s}[n] \geq \mathbf{0}, \mathbf{1}^T\boldsymbol{s}[n] = 1$;
  - $\boldsymbol{\nu}[n]$ is noise; N is the model order.

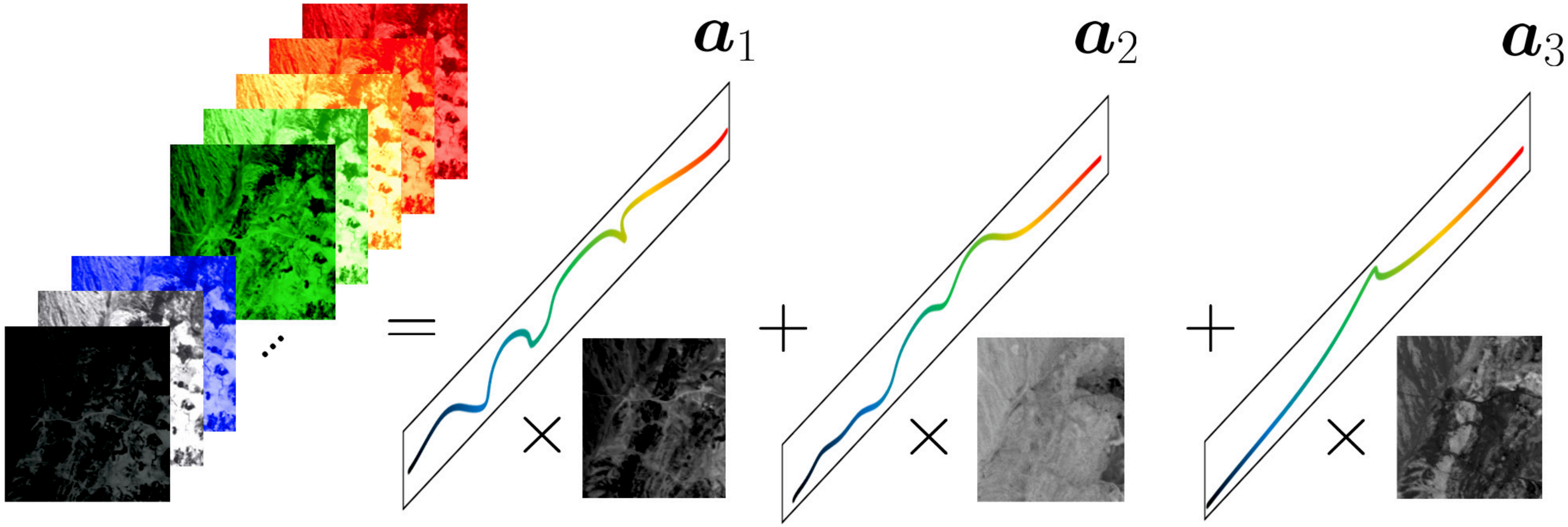

HU: Linear Spectral Mixture Model

- **Model:**

$$\boldsymbol{Y} = \boldsymbol{A}\boldsymbol{S} + \boldsymbol{V}$$

where $\boldsymbol{Y} = [\ \boldsymbol{y}[1], \ldots, \boldsymbol{y}[L]\ ]$; $\boldsymbol{S} = [\ \boldsymbol{s}[1], \ldots, \boldsymbol{s}[L]\ ]$; $\boldsymbol{V} = [\ \boldsymbol{v}[1], \ldots, \boldsymbol{v}[L]\ ]$;
recall $\boldsymbol{s}[n] \geq \boldsymbol{0}, \boldsymbol{1}^T\boldsymbol{s}[n] = 1$

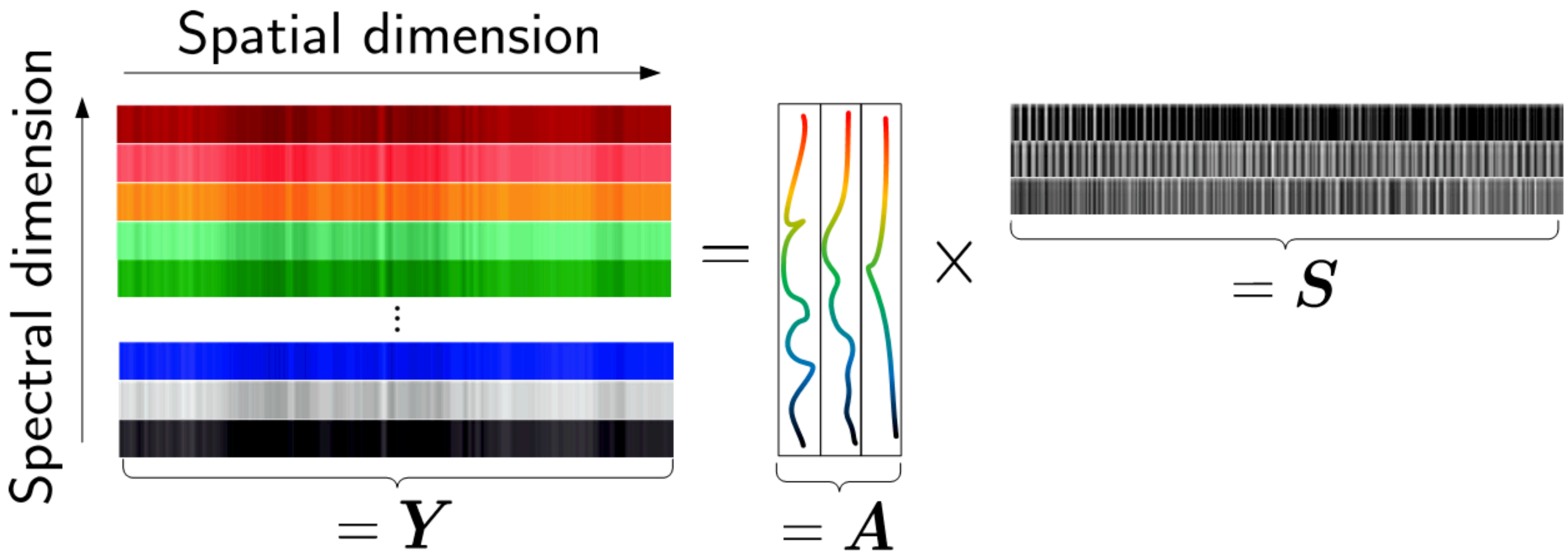

- **HU:** recover $\boldsymbol{A}$ from $\boldsymbol{Y}$
  - once we have $\boldsymbol{A}$ we can get $\boldsymbol{S}$ by $\boldsymbol{S} = \boldsymbol{A}^\dagger\boldsymbol{Y}$

Convex Geometry

Convex Geometry Preliminaries

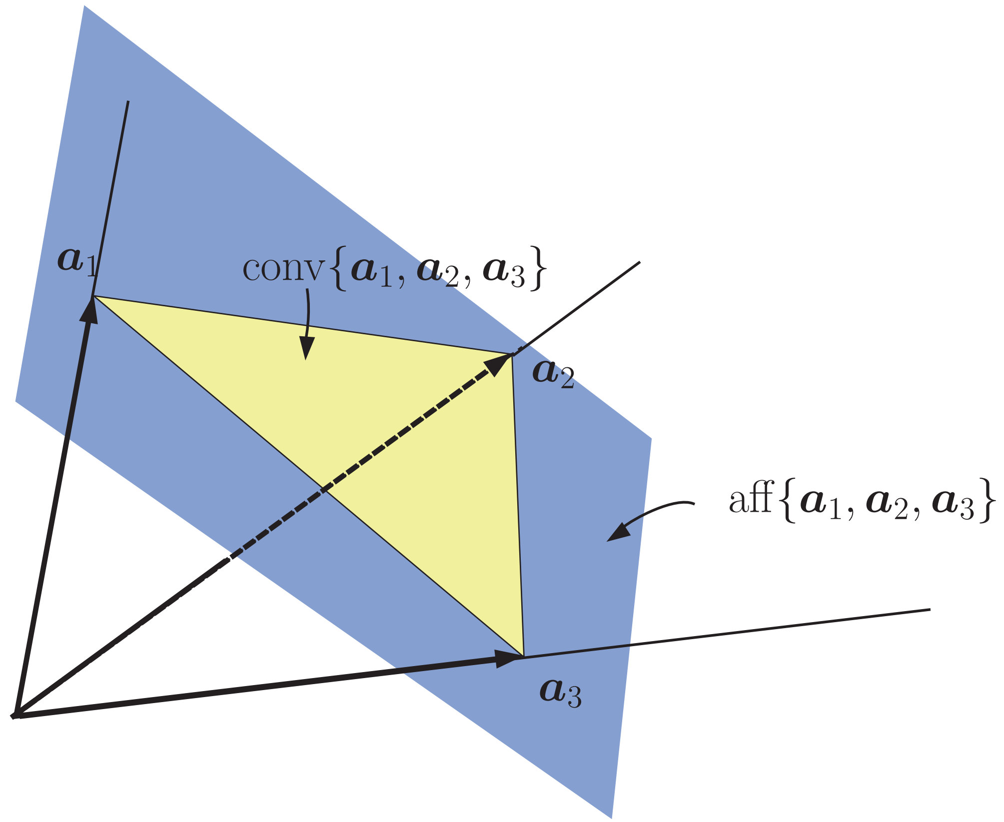

- convex hull: $\text{conv}\{\boldsymbol{a}_1, \ldots, \boldsymbol{a}_N\} = \{\boldsymbol{y} = \sum_{i=1}^{N} \boldsymbol{a}_i \theta_i \mid \boldsymbol{\theta} \geq \boldsymbol{0}, \boldsymbol{1}^T \boldsymbol{\theta} = 1\}$.

- simplex: $\text{conv}\{\boldsymbol{a}_1, \ldots, \boldsymbol{a}_N\}$ is a simplex if $\boldsymbol{a}_1, \ldots, \boldsymbol{a}_N$ are affinely independent.

Convex Geometry Observation

- consider the noiseless model

$$\boldsymbol{y}[n] = \sum_{i=1}^{N} s_i[n]\boldsymbol{a}_i.$$

Since $s_i[n] \geq 0$, $\sum_{i=1}^{N} s_i[n] = 1$,

$$\boldsymbol{y}[n] \in \text{conv}\{\boldsymbol{a}_1, \ldots, \boldsymbol{a}_N\}.$$

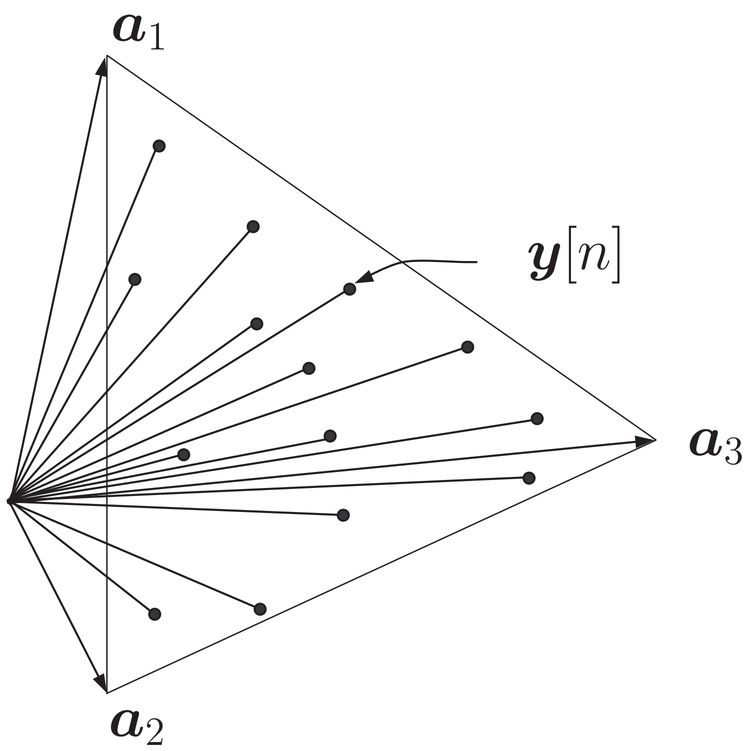

- assume linearly independent $\boldsymbol{a}_1, \ldots, \boldsymbol{a}_N$

- **Observation:** each pixel $\boldsymbol{y}[n]$ lies in the simplex $\text{conv}\{\boldsymbol{a}_1, \ldots, \boldsymbol{a}_N\}$.

Convex Geometry Observation

- consider the noiseless model

$$\boldsymbol{y}[n] = \sum_{i=1}^{N} s_i[n]\boldsymbol{a}_i.$$

Since $s_i[n] \geq 0$, $\sum_{i=1}^{N} s_i[n] = 1$,

$$\boldsymbol{y}[n] \in \text{conv}\{\boldsymbol{a}_1, \ldots, \boldsymbol{a}_N\}.$$

- assume linearly independent $\boldsymbol{a}_1, \ldots, \boldsymbol{a}_N$

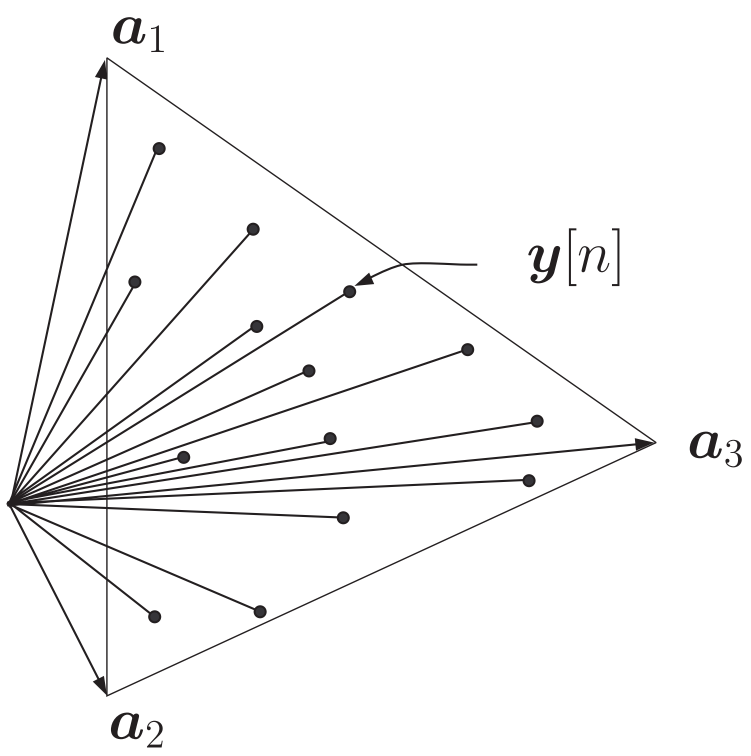

- **Observation:** each pixel $\boldsymbol{y}[n]$ lies in the simplex $\text{conv}\{\boldsymbol{a}_1, \ldots, \boldsymbol{a}_N\}$.

- **Question:** can we identify the vertices of $\text{conv}\{\boldsymbol{a}_1, \ldots, \boldsymbol{a}_N\}$ from $\boldsymbol{y}[1], \ldots, \boldsymbol{y}[L]$?

Craig's Seminal Work [Craig1994]

542 IEEE TRANSACTIONS ON GEOSCIENCE AND REMOTE SENSING, VOL. 32, NO. 3, MAY 1994

Minimum-Volume Transforms for Remotely Sensed Data

Maurice D. Craig

***Abstract*—Scatter diagrams for multispectral remote sensing data tend to be triangular, in the two-band case, pyramidal for three bands, and so on. They radiate away from the so-called darkpoint, which represents the scanner's response to an unilluminated target. A minimum-volume transform may be described (provisionally) as a nonorthogonal linear transformation of the multivariate data to new axes passing through the dark point, with directions chosen such that they (for two bands), or the new coordinate planes (for three bands, etc.) embrace the data cloud as tightly as possible.**

The reason for the observed shapes of scatter diagrams is to be found in the theory of linear mixing at the subfootprint scale. Thus, suitably defined, minimum-volume transforms can often be used to unmix images into new spatial variables showing the proportions of the different cover types present, a type of enhancement that is not only intense, but physically meaningful. The present paper furnishes details for constructing computer programs to effect this operation. It will serve as a convenient technical source that may be referenced in subsequent, more profusely illustrated publications that address the intended application, the mapping of surface mineralogy.

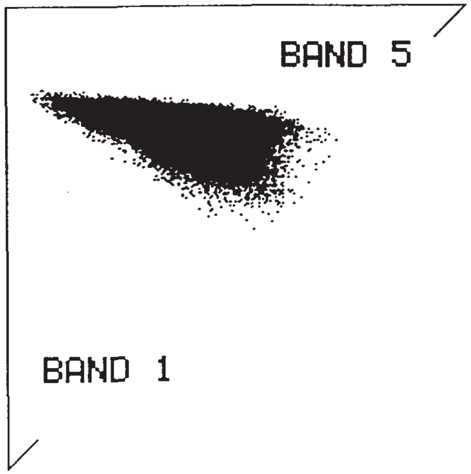

Fig. 1. Two-band triangular scatter plot for a 512 × 512 subscene of a Landsat Thematic Mapper image (actually WRS 111-075, Nullagine, W.A., acquired August 18, 1986).

I. Introduction

THIS paper describes processing algorithms for two closely related transformations, both applicable to radiance data from multispectral scanners. It supplies de-

away from the so-called dark point, the scanner's response to a target of nil reflectance in all bands (see Fig. 1).

This appearance of bivariate scatter diagrams now sug-

Drawing a Connection Between NMF and HU

- consider NMF, which has a model

$$\boldsymbol{z}[n] = \boldsymbol{B}\boldsymbol{c}[n] = \sum_{i=1}^{N} \boldsymbol{b}_i c_i[n], \ n = 1, \ldots, L,$$

  where $\boldsymbol{B} \geq \boldsymbol{0}$, $\boldsymbol{c}[n] \geq \boldsymbol{0}$. We don't have $\boldsymbol{1}^T\boldsymbol{c}[n] = 1$.

- column normalization preprocessing:

$$\boldsymbol{x}[n] = \frac{\boldsymbol{z}[n]}{\boldsymbol{1}^T\boldsymbol{z}[n]} = \sum_{i=1}^{N} \underbrace{\frac{\boldsymbol{b}_i}{\boldsymbol{1}^T\boldsymbol{b}_i}}_{:=\boldsymbol{a}_i} \underbrace{\frac{\boldsymbol{1}^T\boldsymbol{b}_i c_i[n]}{\sum_{i=1}^{N}\boldsymbol{1}^T\boldsymbol{b}_j c_j[n]}}_{:=\boldsymbol{s}_i[n]} = \boldsymbol{A}\boldsymbol{s}[n]$$

- the normalized data points $\boldsymbol{x}[n]$'s adhere to the HU model.
- this means that HU can be applied to NMF through column normalization.

Converting NMF to HU

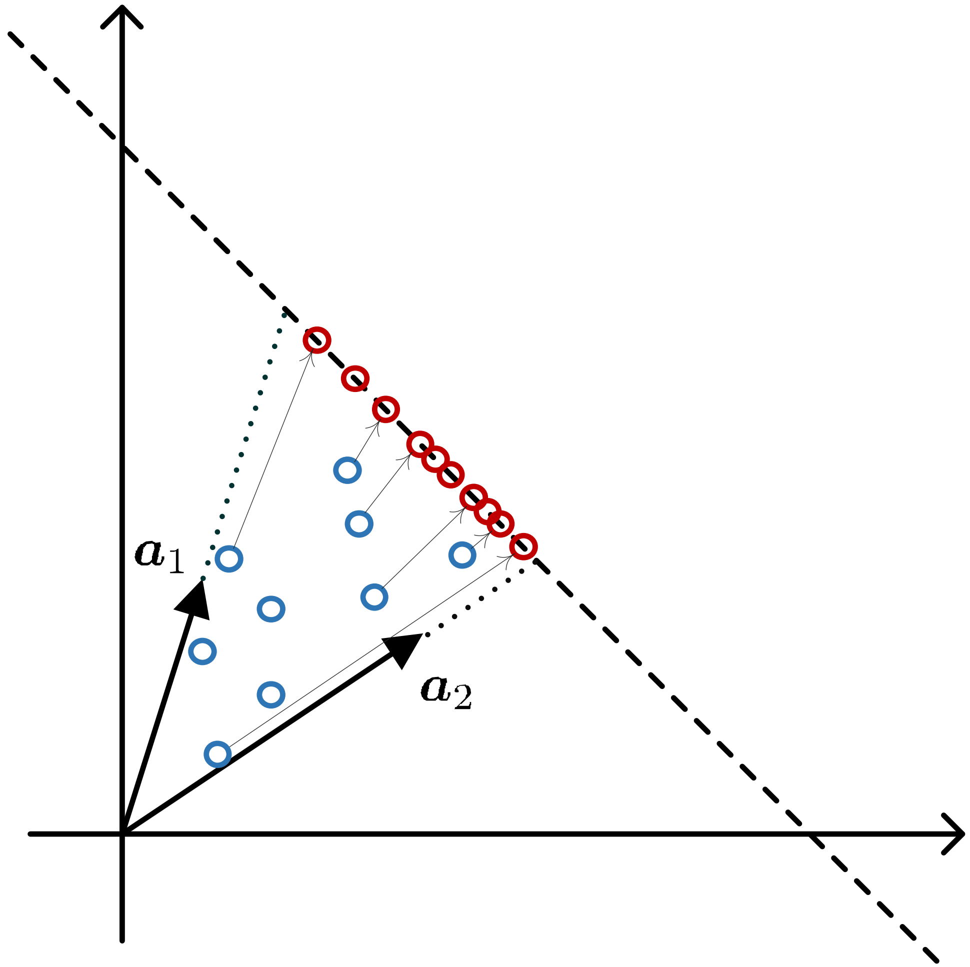

Blue: the original data points $\boldsymbol{z}[n] = \boldsymbol{B}\boldsymbol{c}[n]$. Red: the normalized data points $\boldsymbol{x}[n] = \boldsymbol{z}[n]/(\mathbf{1}^T\boldsymbol{z}[n])$.

Converting NMF to HU

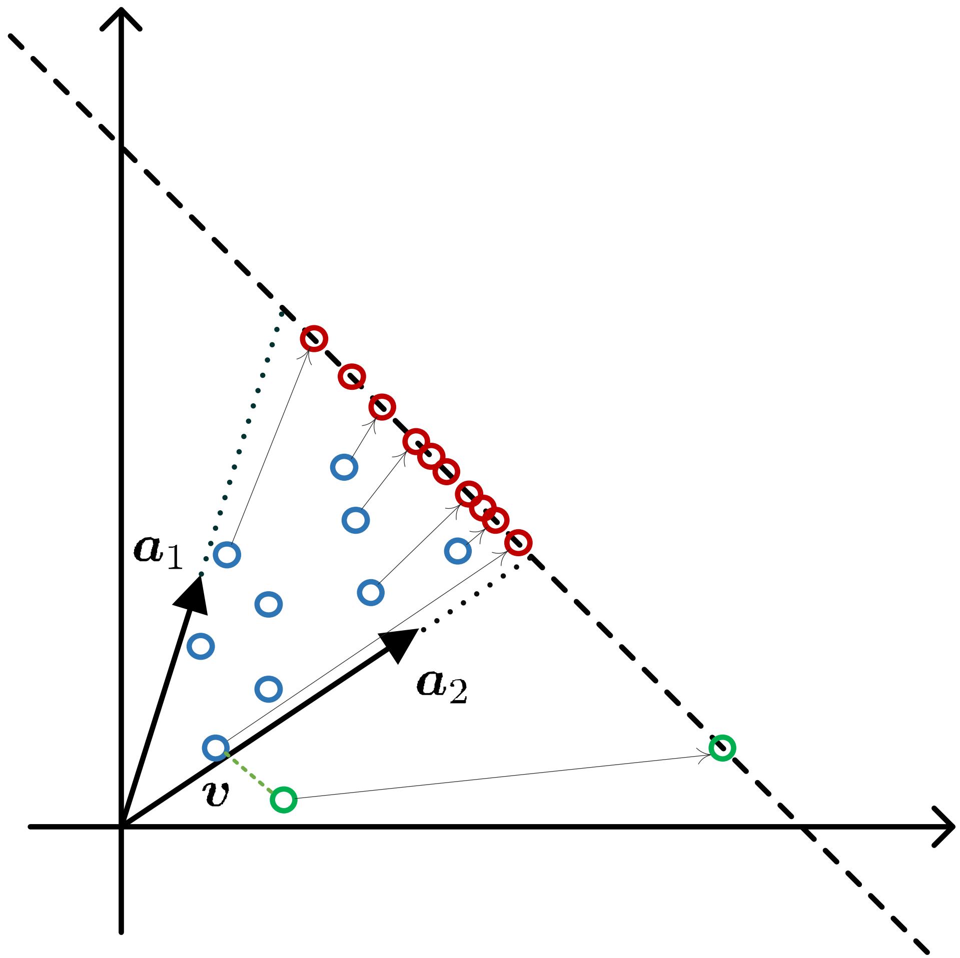

Blue: the original data points $z[n] = Bc[n]$. Red: the normalized data points $x[n] = z[n]/(\mathbf{1}^T z[n])$. Green: a noisy data point.

Pure Pixel Search

Pure Pixels

- **Observation:** there are instances for which some pixels contain only one endmember; you may even read them out manually

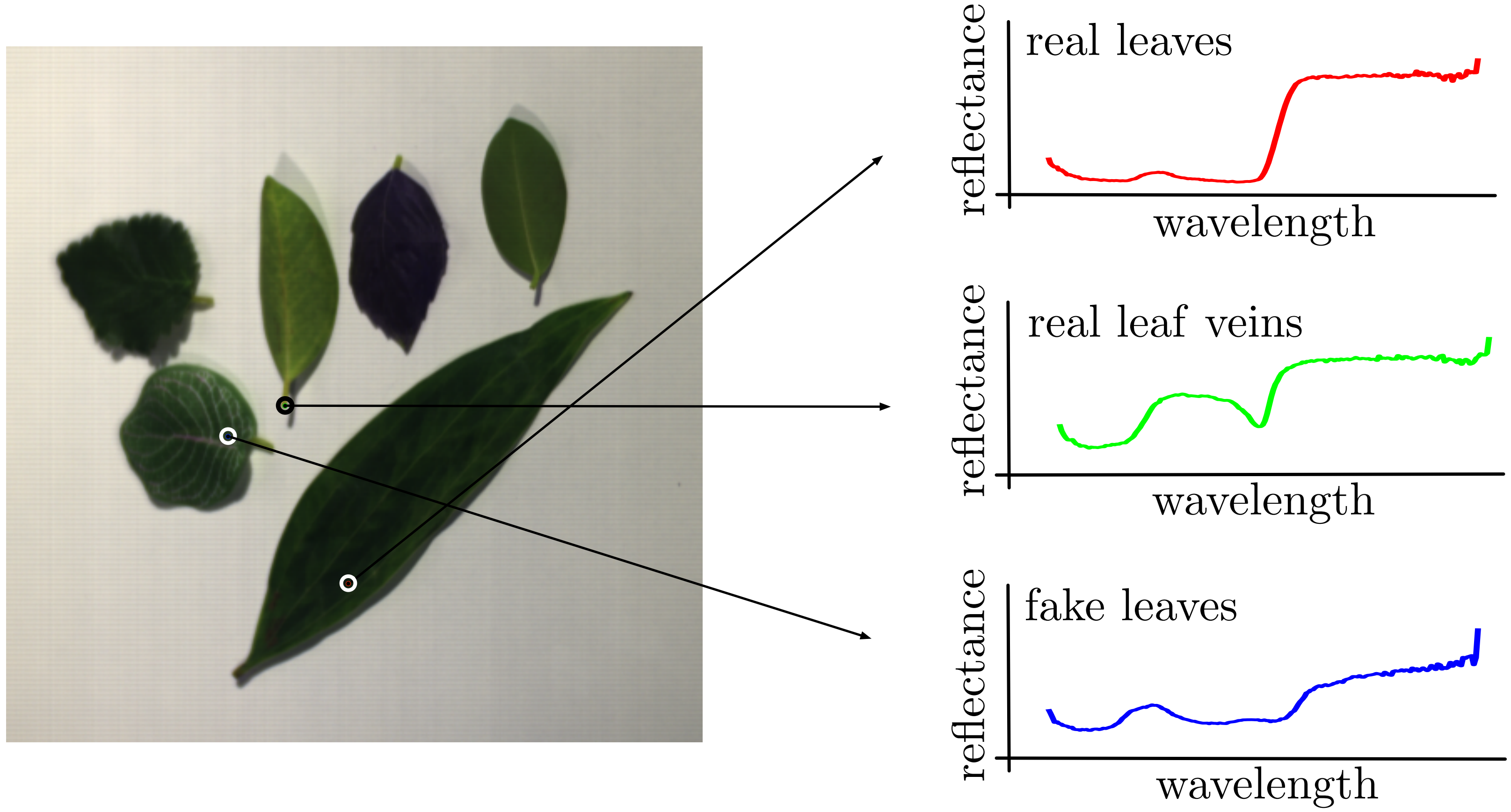

Pure Pixels

Definition: Endmember i is said to have a pure pixel if, without noise, there exists an index ℓ_i such that

$$\boldsymbol{y}[\ell_i] = \boldsymbol{a}_i$$

- or, endmember i has pure pixels if $\boldsymbol{s}[\ell_i] = \boldsymbol{e}_i$ for some ℓ_i; $\boldsymbol{e}_i$'s are unit vectors

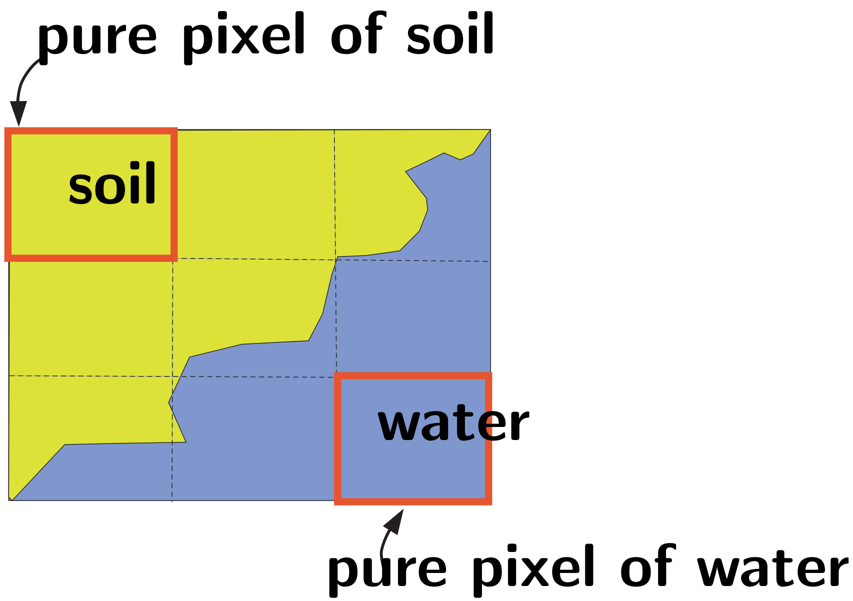

(a) pure pixel case

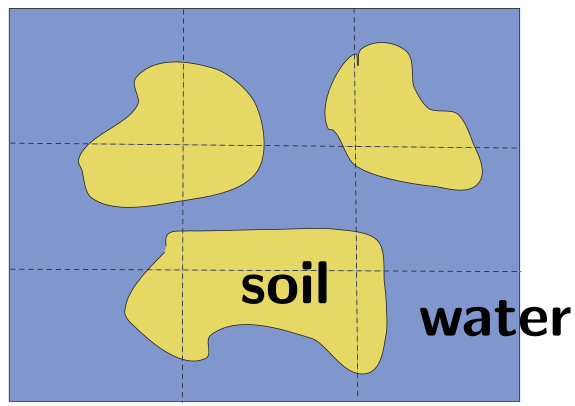

(b) no-pure pixel case

Pure Pixels

Definition: Endmember i is said to have a pure pixel if, without noise, there exists an index ℓ_i such that

$$\boldsymbol{y}[\ell_i] = \boldsymbol{a}_i$$

- **Implication:**
  - Suppose that every endmember has a pure pixel, and there is no noise.
  - If we know $\ell_1, \ldots, \ell_N$, then $[\ \boldsymbol{y}[\ell_1], \ldots, \boldsymbol{y}[\ell_N]\ ] = \boldsymbol{A}$ — and the problem is solved!

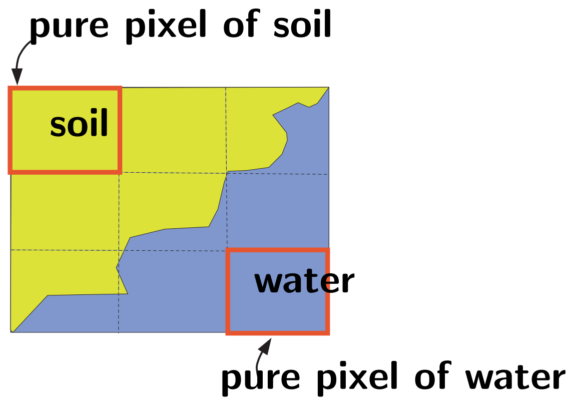

- **Problem:** find the pure pixel indices.

Convex Geometry With and Without Pure Pixels

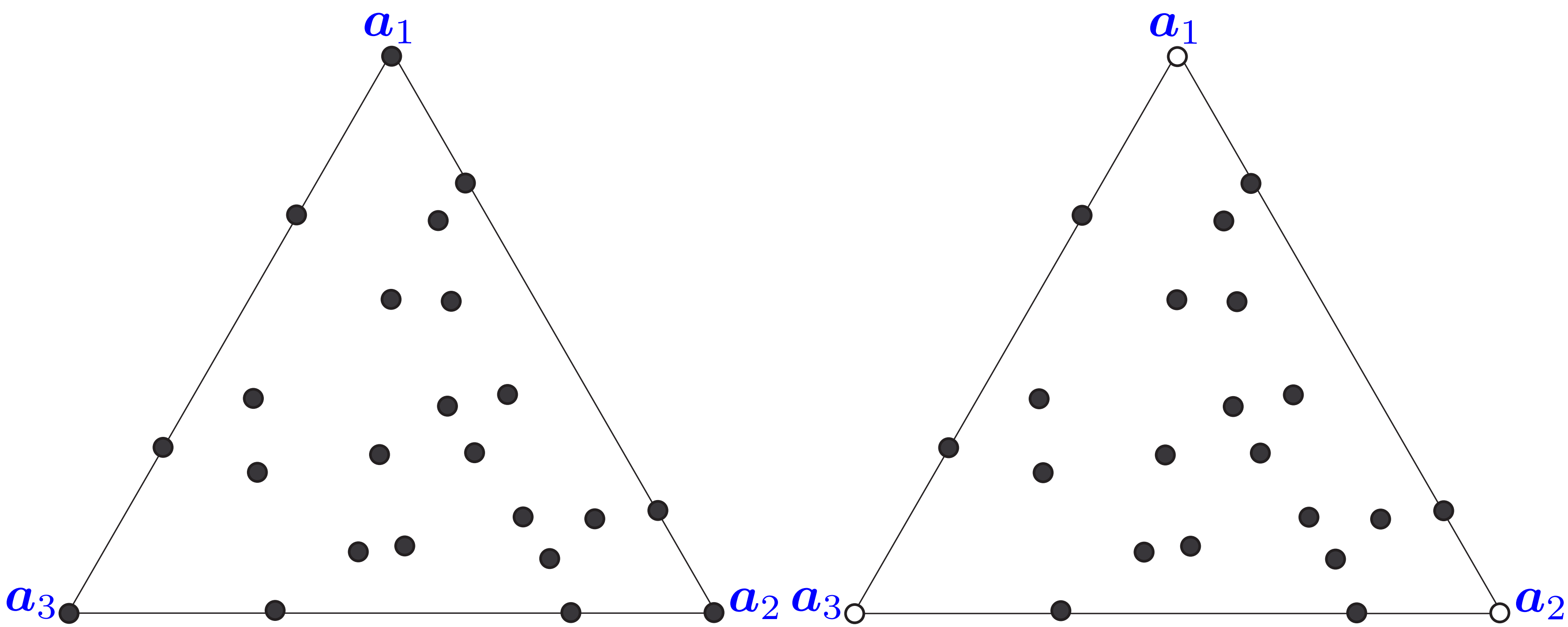

(a) pure pixel case (b) no pure pixel case

- the pure pixel case has points on the vertices
- the no pure pixel case does not.

Successive Projection Algorithm (SPA)

- there are numerous pure pixel search algorithms, e.g.,
  - pure pixel index (PPI) [Boardman-Kruse-Green1995], the first in HU
  - vertex component analysis (VCA) [Nascimento-Bioucas2003], the most popular
- we consider SPA [Gillis-Vavasis2014], arguably the easiest one to understand

A Simple Geometrical Question

Question: the dark dots are the hyperspectral pixels $\boldsymbol{y}[n]$'s. Which $\boldsymbol{y}[n]$ gives the largest Euclidean norm $\|\boldsymbol{y}[n]\|_2$?

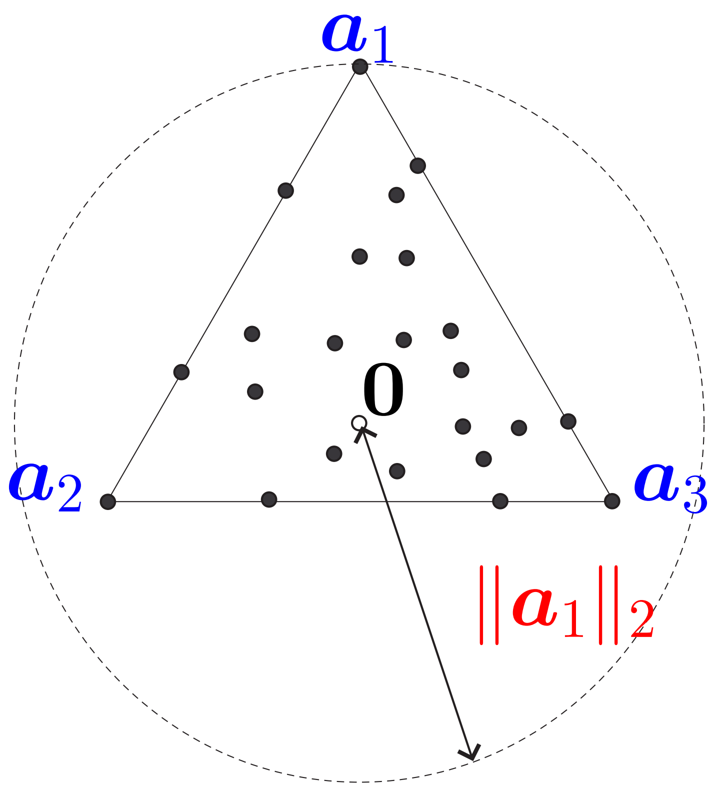

A Simple Geometrical Question

Question: the dark dots are the hyperspectral pixels $\boldsymbol{y}[n]$'s. Which $\boldsymbol{y}[n]$ gives the largest Euclidean norm $\|\boldsymbol{y}[n]\|_2$?

Answer: the pure pixel $\boldsymbol{y}[n] = \boldsymbol{a}_1$ of endmember 1

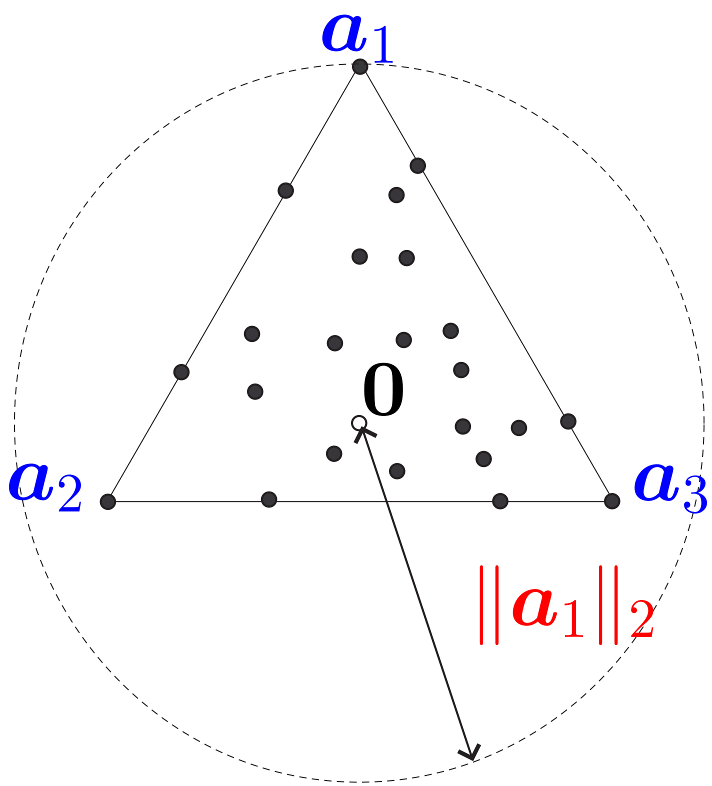

A Simple Geometrical Question

Question: the dark dots are the hyperspectral pixels $\boldsymbol{y}[n]$'s. Which $\boldsymbol{y}[n]$ gives the largest Euclidean norm $\|\boldsymbol{y}[n]\|_2$?

Implication: $\hat{\ell}_1 = \arg \max_{n=1,\ldots,L} \|\boldsymbol{y}[n]\|_2^2$ finds a pure pixel

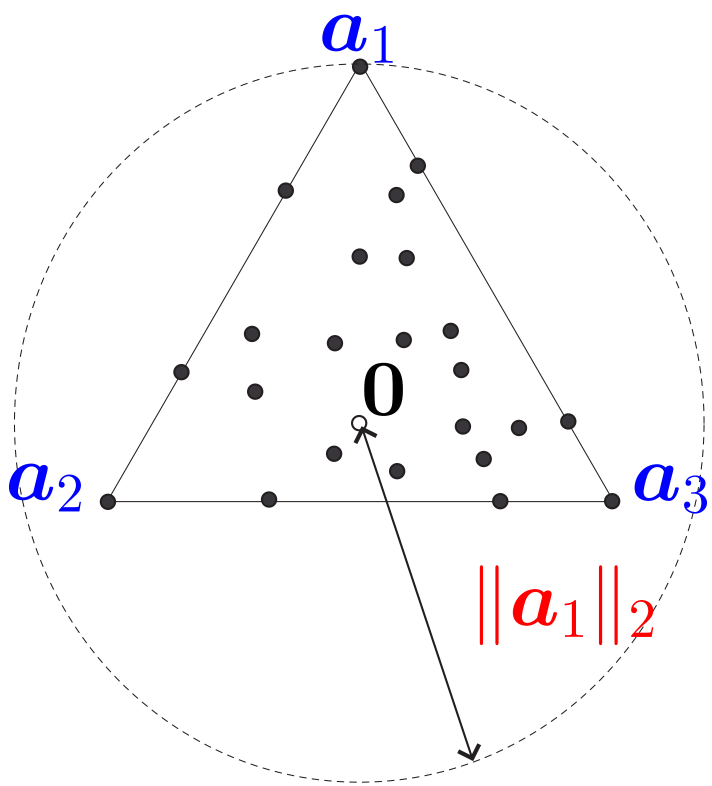

Another Simple Geometrical Question

Question: suppose that $\boldsymbol{a}_1$ is known and we project $\boldsymbol{y}[n]$'s onto a line perpendicular to $\boldsymbol{a}_1$. Which $\boldsymbol{y}[n]$ has the largest Euclidean norm on that line?

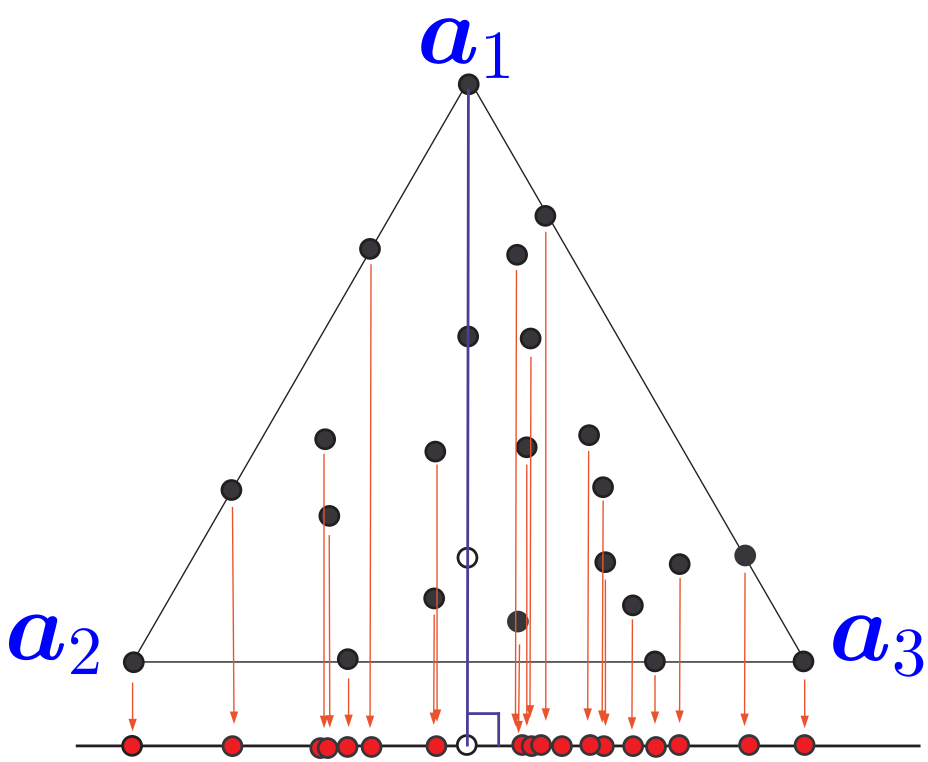

Another Simple Geometrical Question

Question: suppose that $\boldsymbol{a}_1$ is known and we project $\boldsymbol{y}[n]$'s onto a line perpendicular to $\boldsymbol{a}_1$. Which $\boldsymbol{y}[n]$ has the largest Euclidean norm on that line?

Answer: either the pure pixel $\boldsymbol{y}[n] = \boldsymbol{a}_2$ or $\boldsymbol{y}[n] = \boldsymbol{a}_3$

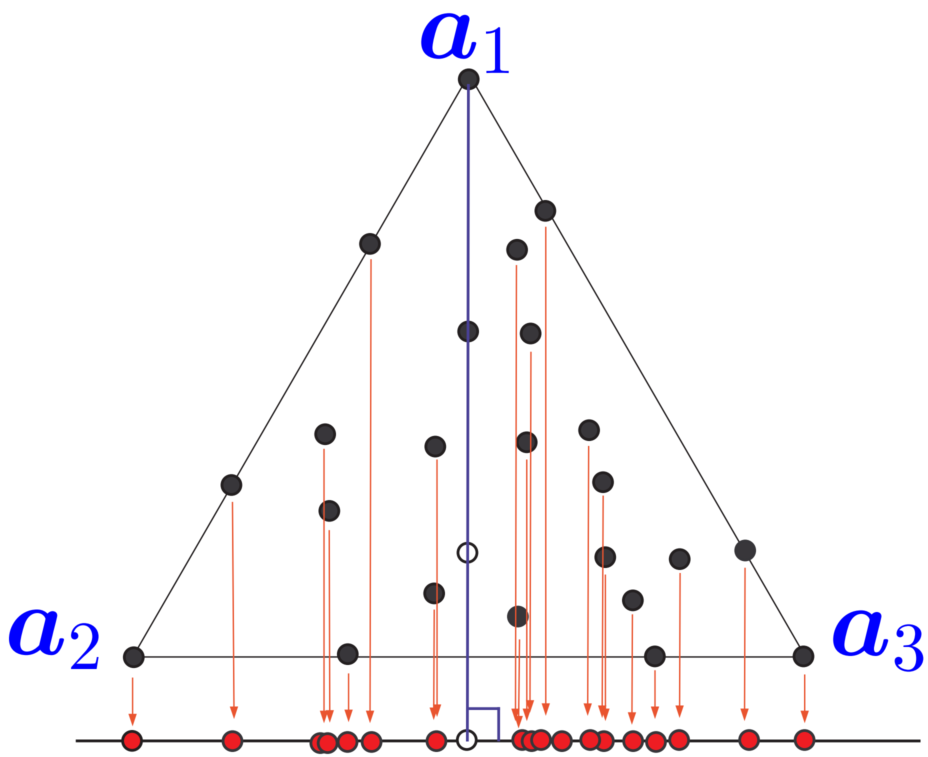

Another Simple Geometrical Question

Question: suppose that $\boldsymbol{a}_1$ is known and we project $\boldsymbol{y}[n]$'s onto a line perpendicular to $\boldsymbol{a}_1$. Which $\boldsymbol{y}[n]$ has the largest Euclidean norm on that line?

Implication: $\hat{\ell}_2 = \arg \max_{n=1,\ldots,L} \|\boldsymbol{P}_{\boldsymbol{a}_1}^{\perp}\boldsymbol{y}[n]\|_2^2$, where $\boldsymbol{P}_{\boldsymbol{a}_1}^{\perp} = \boldsymbol{I} - \boldsymbol{a}_1\boldsymbol{a}_1^T/\|\boldsymbol{a}_1\|_2^2$ is the orthogonal complement projector of $\boldsymbol{a}_1$, finds a pure pixel

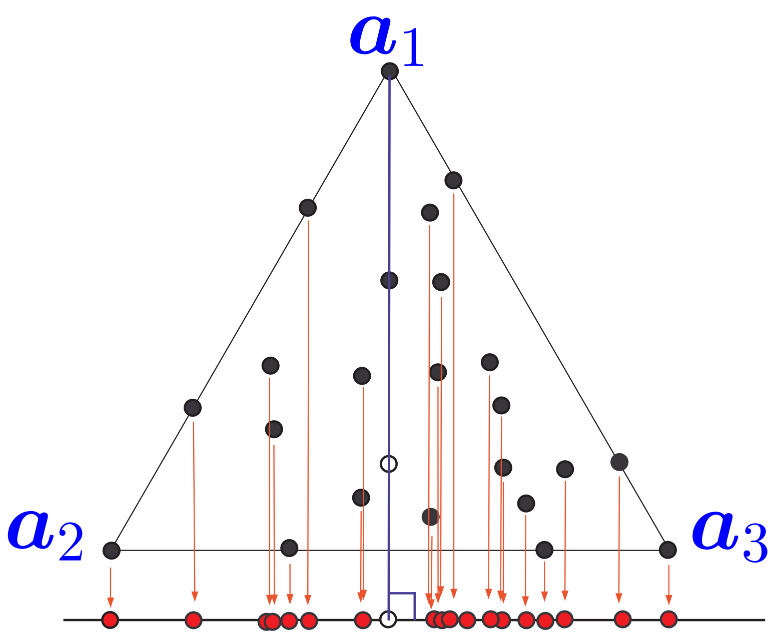

Successive Projection Algorithm (SPA)

Algorithm: SPA
input $\{\boldsymbol{y}[n]\}_{n=1}^{L}$, N.
$\hat{\ell}_1 = \arg \max_{n=1,\ldots,L} \|\boldsymbol{y}[n]\|_2^2$. % find the pixel with the largest Euclidean norm
$\hat{\boldsymbol{A}} = \boldsymbol{y}[\hat{\ell}_1]$.
for $k = 2, \ldots, N$
    % project pixels onto the orthogonal complement subspace of $\hat{\boldsymbol{A}}$, and find the projected pixel with the largest Euclidean norm
    $\hat{\ell}_k = \arg \max_{n=1,\ldots,L} \|\boldsymbol{P}_{\hat{\boldsymbol{A}}}^{\perp}\boldsymbol{y}[n]\|_2^2$, where $\boldsymbol{P}_{\hat{\boldsymbol{A}}}^{\perp} = \boldsymbol{I} - \hat{\boldsymbol{A}}(\hat{\boldsymbol{A}}^T\hat{\boldsymbol{A}})^{-1}\hat{\boldsymbol{A}}^T$
    $\hat{\boldsymbol{A}} := [\ \hat{\boldsymbol{A}},\ \boldsymbol{y}[\hat{\ell}_k]\ ]$.
end
output $\hat{\boldsymbol{A}}$.

- simple algorithm; computationally cheap

SPA is Theoretically Interesting

- guarantee exact recovery in the noiseless case [Chan-Ma-Ambikapathi-Chi2011]

> **Fact**: If the pure pixel assumption holds and $\boldsymbol{a}_1, \ldots, \boldsymbol{a}_N$ are linearly independent, SPA recovers $\boldsymbol{a}_1, \ldots, \boldsymbol{a}_N$ exactly in the noiseless case.

- shown to be robust to noise [Gillis-Vavasis2014]

> **Theorem**: If the pure pixel assumption holds and the noise level $\epsilon = \max_{n=1,\ldots,L} \|\boldsymbol{\nu}[n]\|_2$ is sufficient small, SPA recovers $\boldsymbol{a}_1, \ldots, \boldsymbol{a}_N$ up to error $\mathcal{O}(\epsilon\kappa(\boldsymbol{A})^2)$ where $\kappa(\boldsymbol{A})$ is the condition number of $\boldsymbol{A}$.

- many extensions (with provable guarantees), has tight connections to simplex volume maximization [Chan-Ma-Ambikapathi-Chi2011] and self-dictionary sparse regression [Fu-Ma-Chan-Bioucas2015]

A Self-Dictionary Example:
Video Summarization in Computer Vision

The video summarization result shown in [Elhamifar-Sapiro-Vidal2012]. Courtesy to the above reference.

- **Problem:** find a (small) subset of video frames that best represents the whole set of video frames.

Self-Dictionary Sparse Regression

- **Problem:** use a smallest subset of measurements to represent all measurements

$$\min_{\boldsymbol{C}} \|\boldsymbol{C}\|_{\text{row}-0}$$
$$\text{s.t. } \boldsymbol{Y} = \boldsymbol{Y}\boldsymbol{C},\ \boldsymbol{C} \geq \boldsymbol{0},\ \boldsymbol{1}^T\boldsymbol{C} = \boldsymbol{1}^T,$$

where $\|\boldsymbol{C}\|_{\text{row}-0}$ counts the number of nonzero rows of $\boldsymbol{C}$.

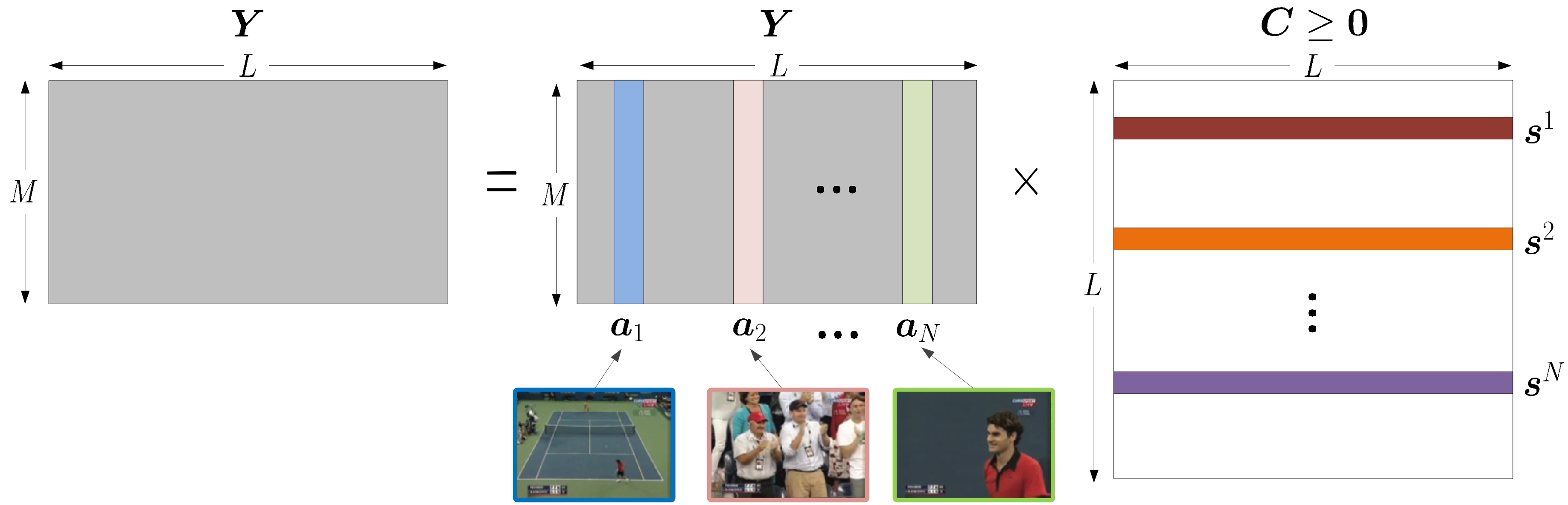

Self-Dictionary Sparse Regression

- **Problem:** use a smallest subset of measurements to represent all measurements

$$\min_{\boldsymbol{C}} \|\boldsymbol{C}\|_{\text{row}-0}$$
$$\text{s.t. } \boldsymbol{Y} = \boldsymbol{Y}\boldsymbol{C},\ \boldsymbol{C} \geq \boldsymbol{0},\ \boldsymbol{1}^T\boldsymbol{C} = \boldsymbol{1}^T.$$

- turns out to be equivalent to pure pixel search— but without requiring knowledge of N [Esser-Moller-Osher-Sapiro-Xin2012]

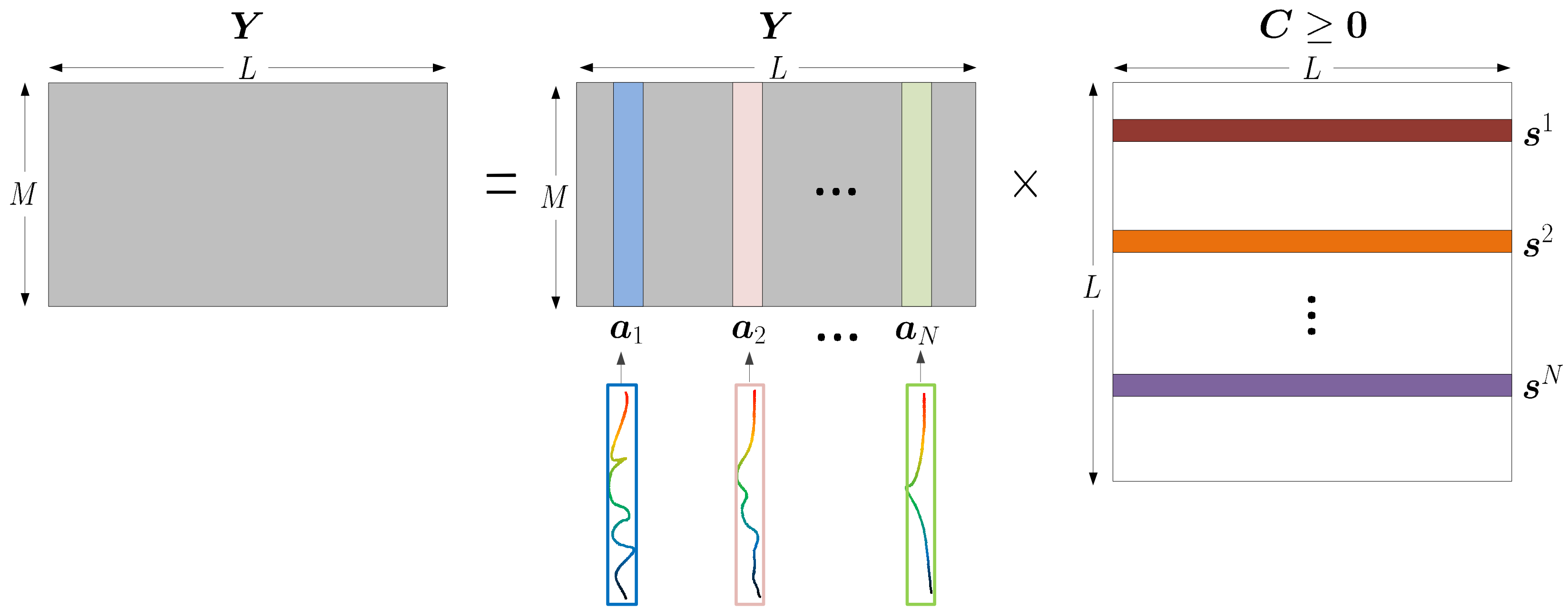

Self-Dictionary Sparse Regression

- **Problem:** use a smallest subset of measurements to represent all measurements

$$
\begin{aligned}
&\min_{\boldsymbol{C}} \ \|\boldsymbol{C}\|_{\text{row}-0} \\
&\text{s.t. } \boldsymbol{Y} = \boldsymbol{Y}\boldsymbol{C}, \ \boldsymbol{C} \geq \boldsymbol{0}, \ \boldsymbol{1}^T\boldsymbol{C} = \boldsymbol{1}^T.
\end{aligned}
$$

- same as separable NMF for topic modeling [Arora-Ge-Kannan-Moitra2012]; the separability assumption is the same as the pure pixel assumption

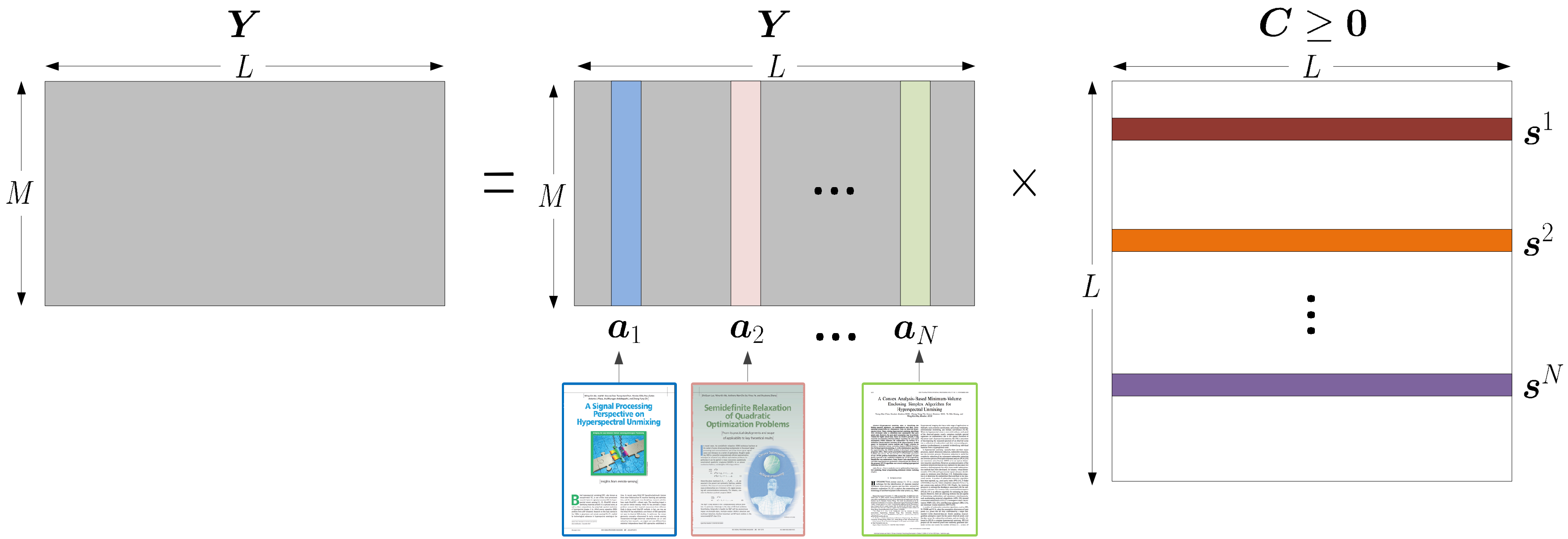

Self-Dictionary Sparse Regression

- **Problem:**

$$\min_{\boldsymbol{C}} \|\boldsymbol{C}\|_{\text{row}-0}$$
$$\text{s.t. } \boldsymbol{Y} = \boldsymbol{Y}\boldsymbol{C}, \ \boldsymbol{C} \geq \boldsymbol{0}, \ \boldsymbol{1}^T\boldsymbol{C} = \boldsymbol{1}^T.$$

- how to (approximately) solve this problem?
  - convex relaxation: approximate $\|\cdot\|_{\text{row}-0}$ by a convex function, such as $\|\boldsymbol{C}\|_{2,1} = \sum_j \|\boldsymbol{c}^j\|_2$
  - references: [Esser-Moller-Osher-Sapiro-Xin2012], [Elhamifar-Sapiro-Vidal2012], [Recht-Re-Tropp-Bittorf2012], and more...

Self-Dictionary Sparse Regression

- **Problem:**

$$\min_{\boldsymbol{C}} \|\boldsymbol{C}\|_{\mathrm{row}-0}$$
$$\text{s.t. } \boldsymbol{Y} = \boldsymbol{Y}\boldsymbol{C},\ \boldsymbol{C} \geq \mathbf{0},\ \mathbf{1}^T\boldsymbol{C} = \mathbf{1}^T.$$

- how to (approximately) solve this problem?
  - greedy pursuit: greedily picks one atom at a time, and repeat

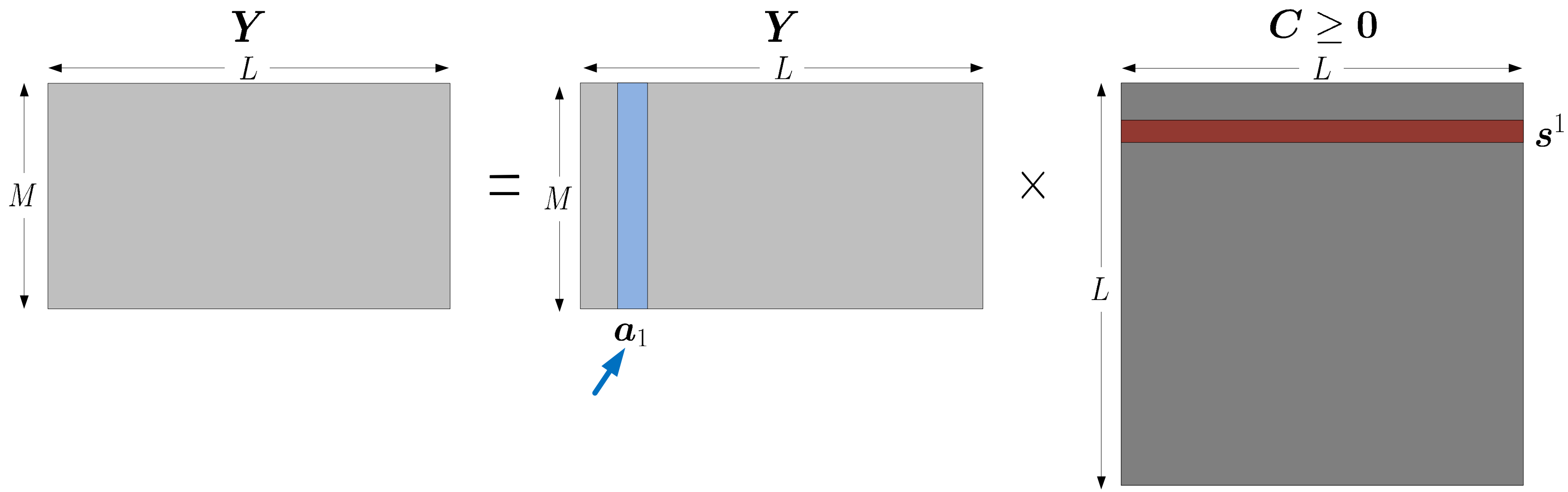

Self-Dictionary Sparse Regression

- **Problem:**

$$\min_{\boldsymbol{C}} \|\boldsymbol{C}\|_{\text{row}-0}$$
$$\text{s.t. } \boldsymbol{Y} = \boldsymbol{Y}\boldsymbol{C},\ \boldsymbol{C} \geq \boldsymbol{0},\ \boldsymbol{1}^T\boldsymbol{C} = \boldsymbol{1}^T.$$

- how to (approximately) solve this problem?
  - greedy pursuit: greedily picks one atom at a time, and repeat

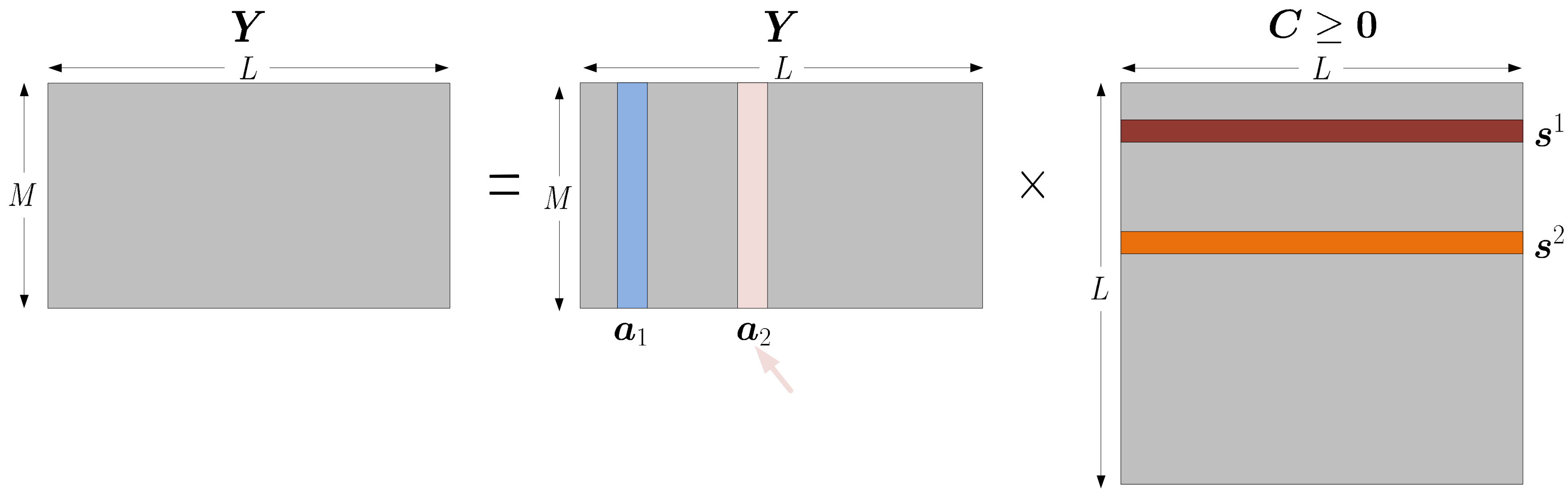

Self-Dictionary Sparse Regression

- **Problem:**

$$\min_{\boldsymbol{C}} \|\boldsymbol{C}\|_{\text{row}-0}$$
$$\text{s.t. } \boldsymbol{Y} = \boldsymbol{Y}\boldsymbol{C},\ \boldsymbol{C} \geq \boldsymbol{0},\ \boldsymbol{1}^T\boldsymbol{C} = \boldsymbol{1}^T.$$

- how to (approximately) solve this problem?
  - greedy pursuit: greedily picks one atom at a time, and repeat

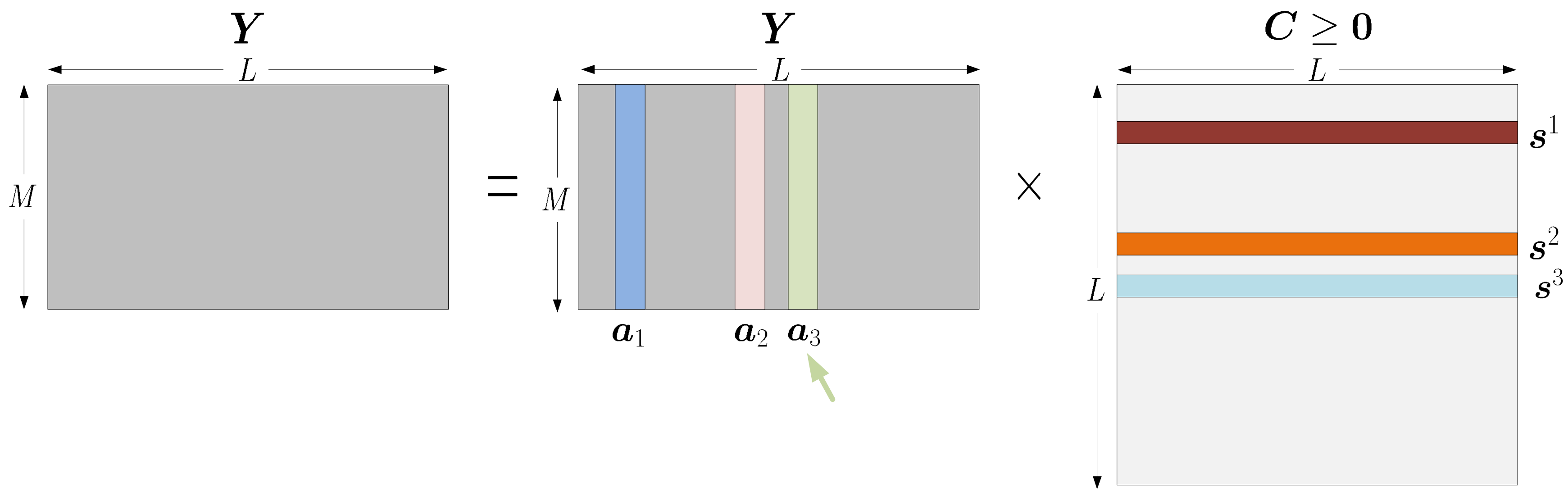

Self-Dictionary Sparse Regression

- **Problem:**

$$\min_{\boldsymbol{C}} \|\boldsymbol{C}\|_{\text{row}-0}$$
$$\text{s.t. } \boldsymbol{Y} = \boldsymbol{Y}\boldsymbol{C},\ \boldsymbol{C} \geq \boldsymbol{0},\ \boldsymbol{1}^T\boldsymbol{C} = \boldsymbol{1}^T.$$

- how to (approximately) solve this problem?
  - greedy pursuit: one instance of greedy pursuit, simultaneous orthogonal matching pursuit, is the same as SPA [Fu-Ma-Chan-Bioucas2015]

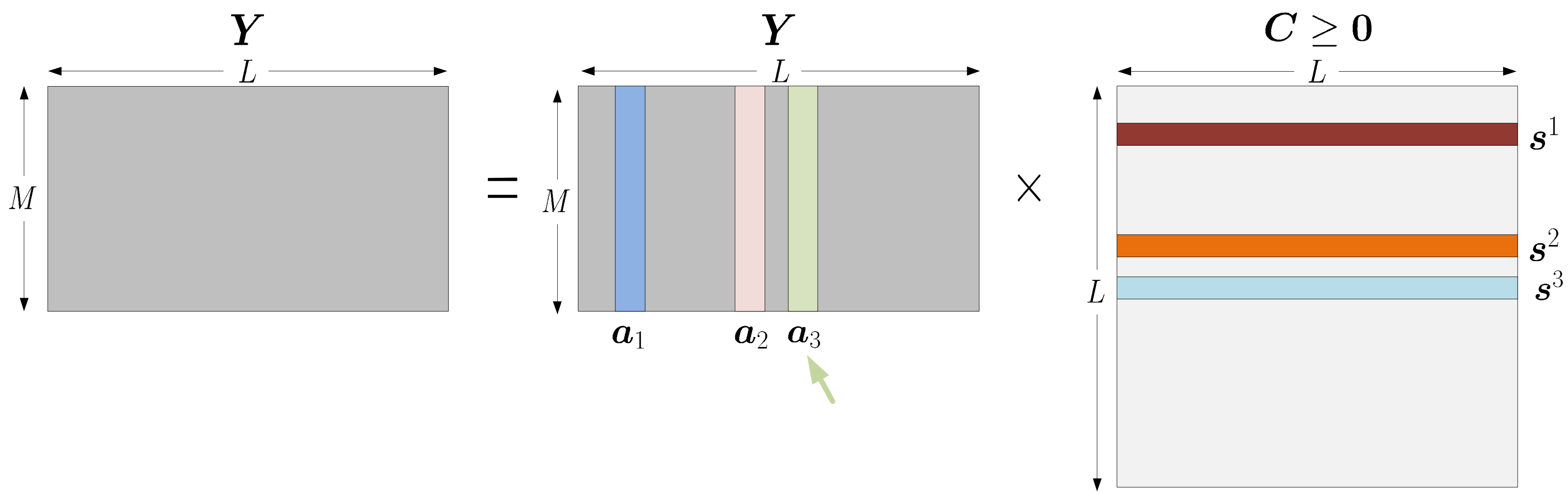

Applications Beyond HU Itself

Who Invented Convex Geometry?

- Craig is most widely recognized for introducing CG in hyperspectral remote sensing [Craig1990], [Craig1994]
  - worth mentioning: Boardman and Winter for pioneering pure pixel search [Boardman-Kruse-Green1995], [Winter1999]

- intriguingly, CG has been discovered or rediscovered several times in other fields
  - geology [Imbrie1964], also [Full-Ehrlich-Klovan1981]
  - chemometrics [Perczel et al. 1989]
  - nuclear magnetic resonance spectroscopy [Naanaa-Nuzillard2005]
  - signal processing theory and methods [Chan-Ma-Chi-Wang2008]
  - (in a way) machine learning [Arora-Ge-Kannan-Moitra2012]

Applications Beyond HU

- machine learning and data science: topic modeling, as mentioned; community detection; crowdsourcing
- biomedical imaging
- signal processing: classical blind source separation
- remote sensing: hyperspectral super-resolution
- many more...

Dynamic Fluorescent Imaging (DFI) and My CG in 2008

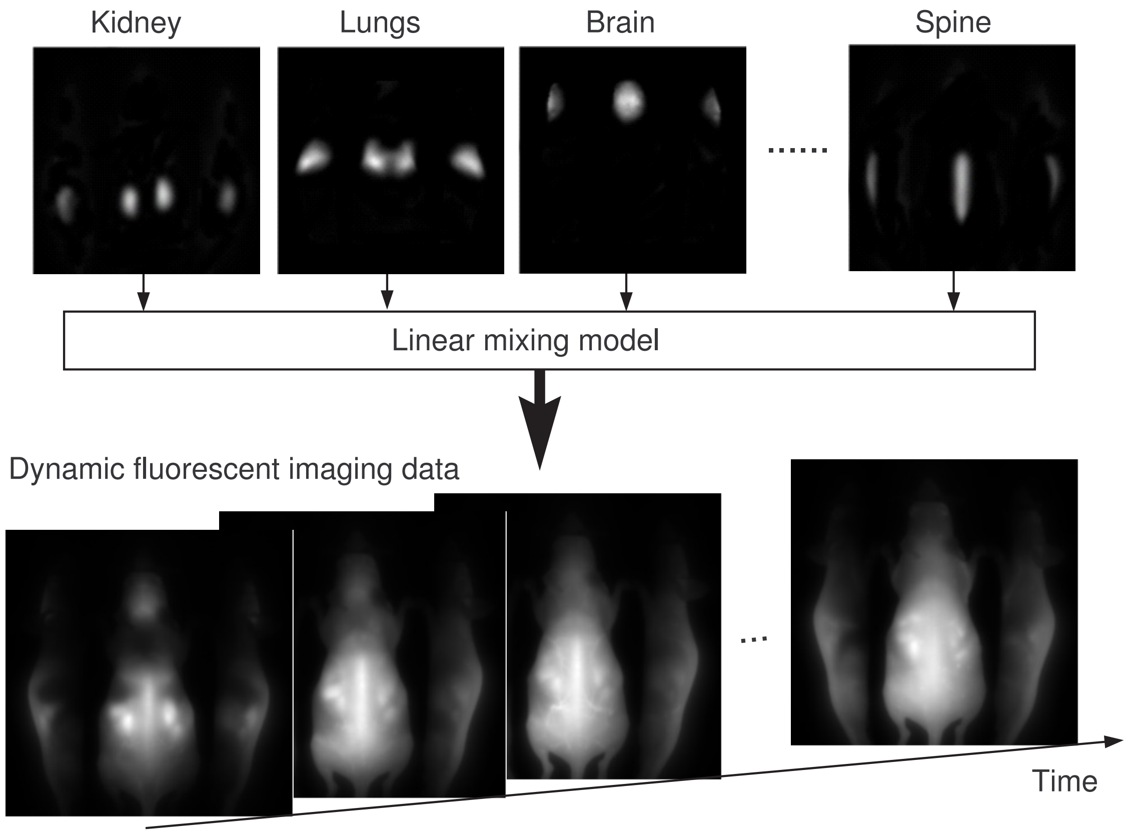

- DFI images are linear mixtures of the anatomical maps of different organs
- model: $\boldsymbol{y}[n] = \boldsymbol{A}\boldsymbol{s}[n]$, $\boldsymbol{s}[n] \geq \boldsymbol{0}$, $\boldsymbol{1}^T\boldsymbol{A} = \boldsymbol{1}^T$ (not $\boldsymbol{1}^T\boldsymbol{s}[n] = 1$ as in HU)

DFI and My CG in 2008

DFI and My CG in 2008

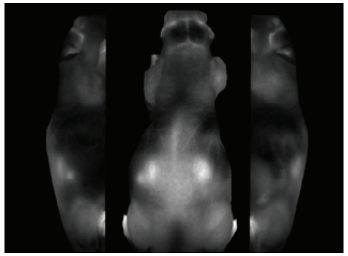

Kidney

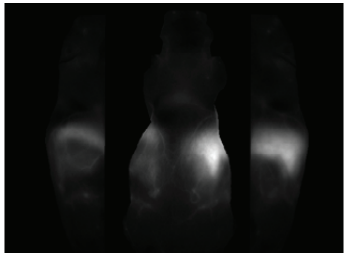

Liver

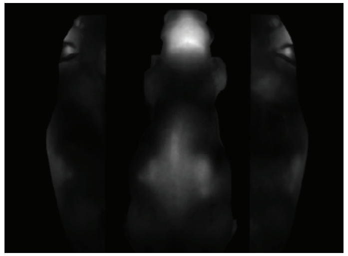

Brain

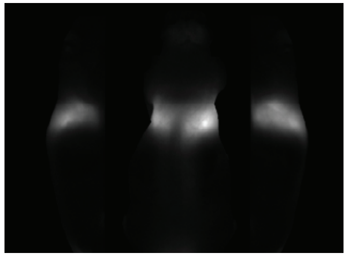

Lung

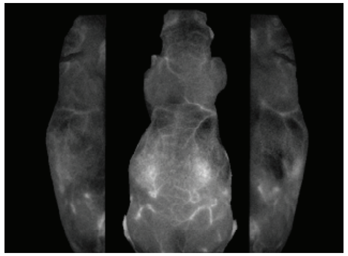

Blood vessels

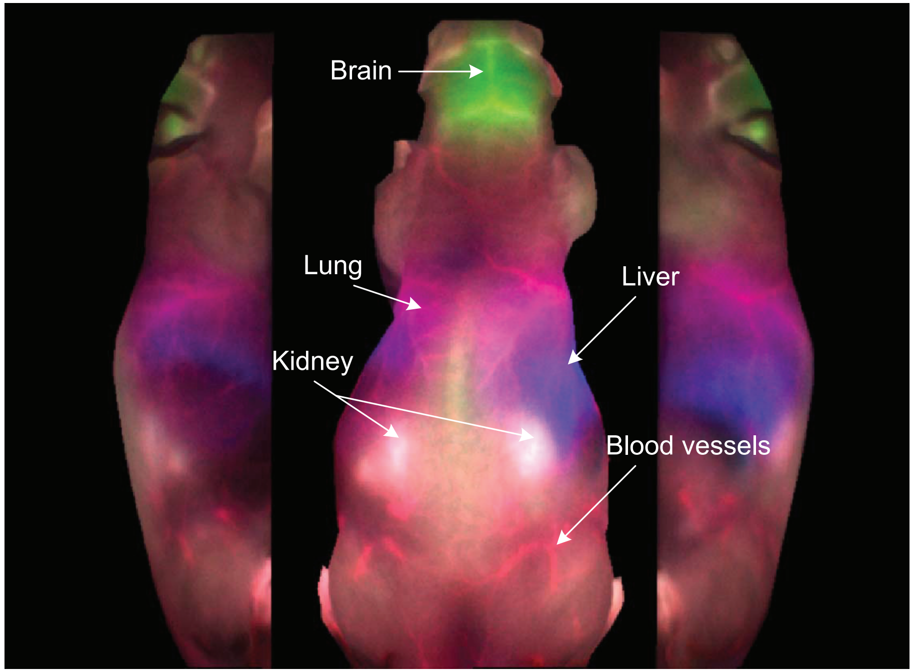

Anatomical map

- anatomical maps recovered by a CG method [Chan-Ma-Chi-Wang2008]

Blind Source Separation (BSS)

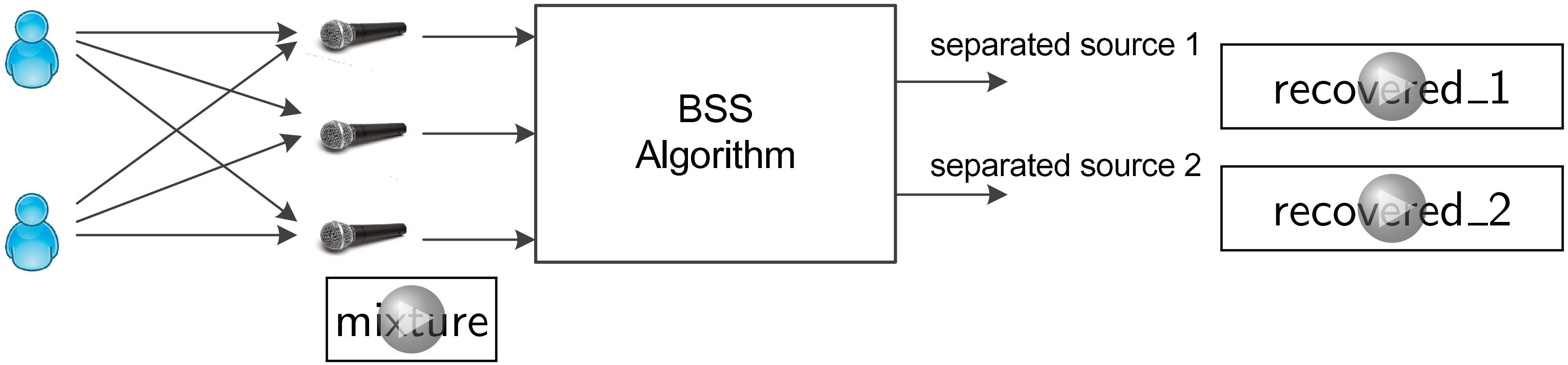

- a classic problem in signal processing, similar model and problem statement as HU

- can we apply convex geometry to BSS?

Pure Pixels and Classical BSS

- Our work in [Fu-Ma-Huang-Sidiropoulos2015]:
  - hypothesis: existence of pure short-time frames; reasonable for speech
  - formulation: a tensor factorization problem with one factor having pure pixels

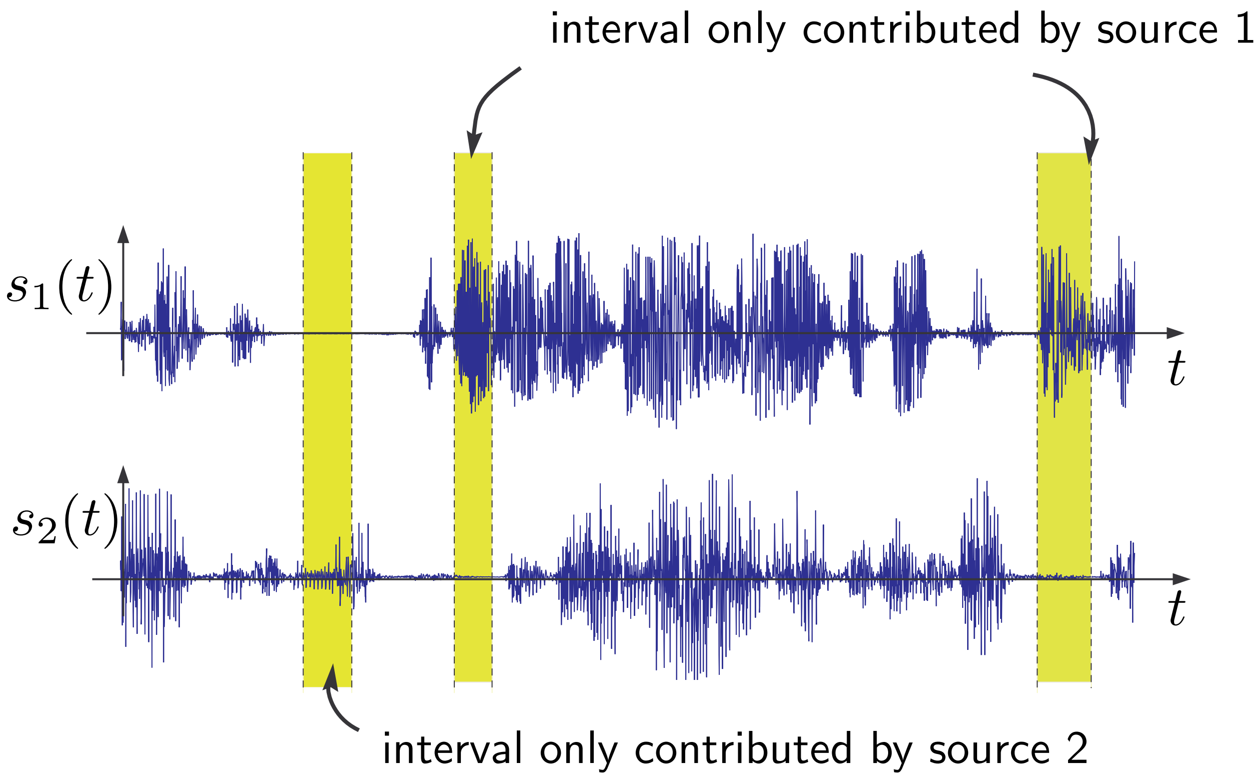

Pure Pixels and Classical BSS

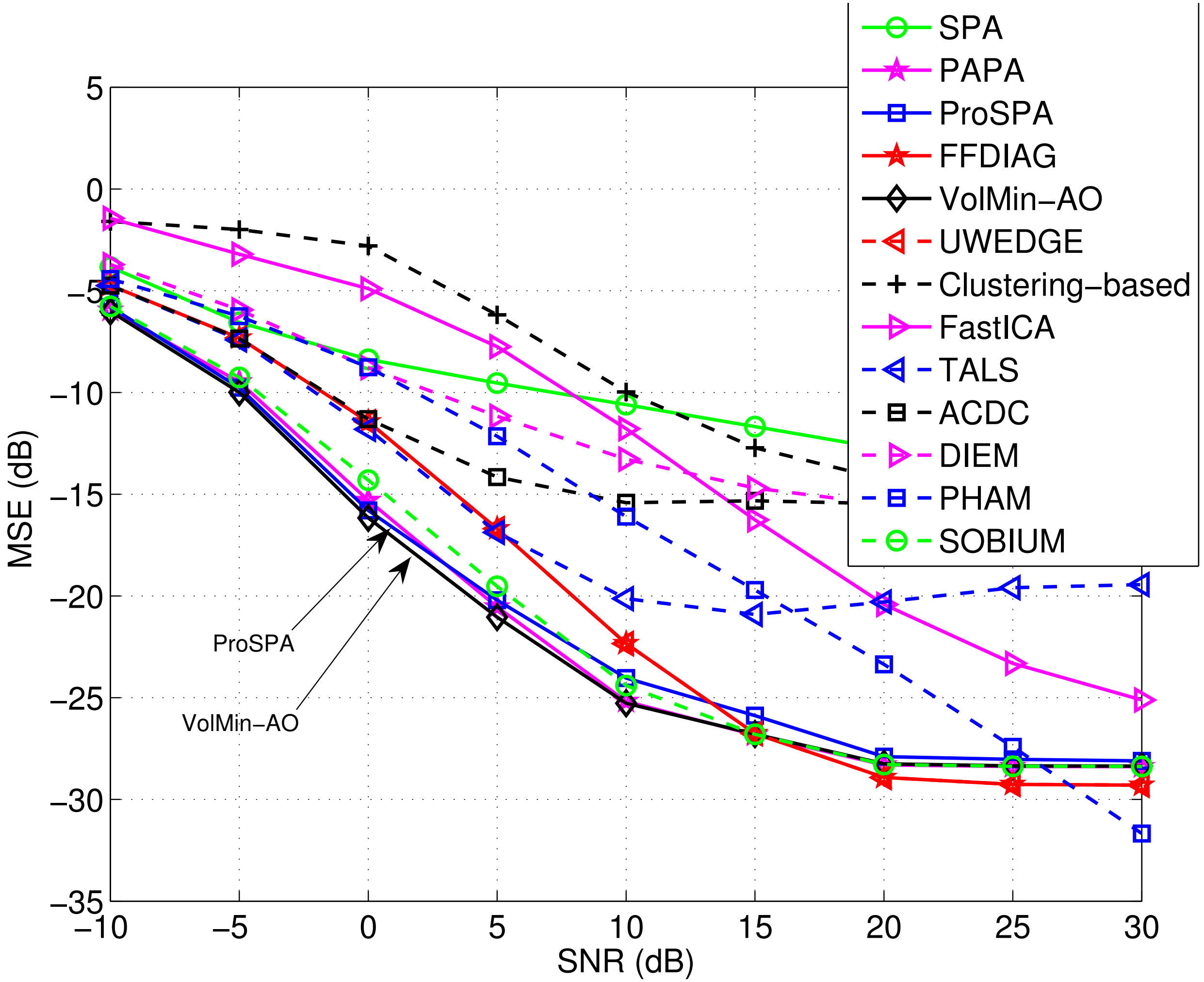

Performance comparison of various BSS algorithms. 'ProSPA' is a modified version of SPA, custom-designed for the blind speech separation application.

Simplex Volume Minimization

Simplex Volume Minimization: Intuition

Craig's belief [Craig1994]: the true endmembers may be located by finding a data enclosing simplex whose volume is the smallest.

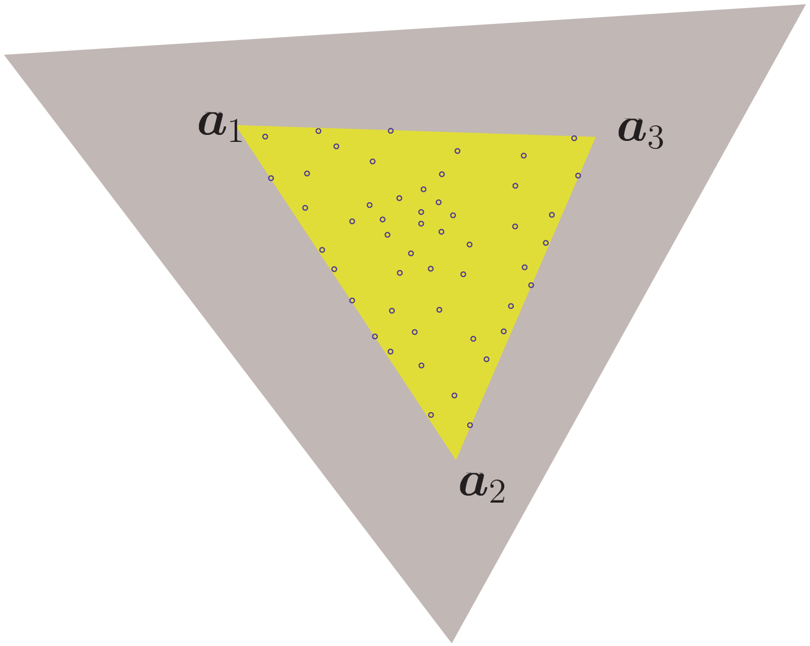

Simplex Volume Minimization: Intuition

Craig's belief [Craig1994]: the true endmembers may be located by finding a data enclosing simplex whose volume is the smallest.

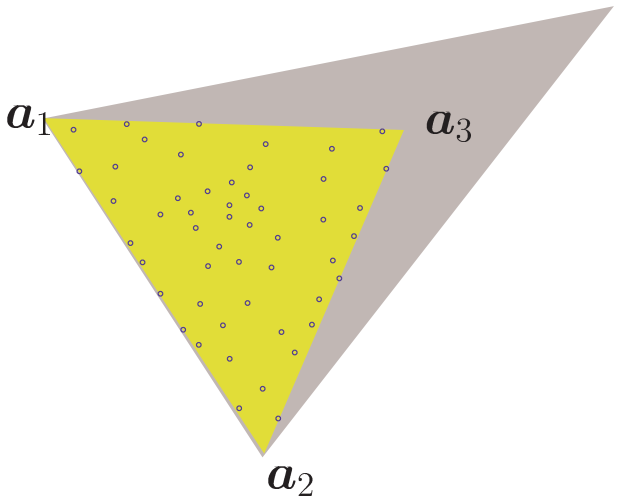

Simplex Volume Minimization: Intuition

Craig's belief [Craig1994]: the true endmembers may be located by finding a data enclosing simplex whose volume is the smallest.

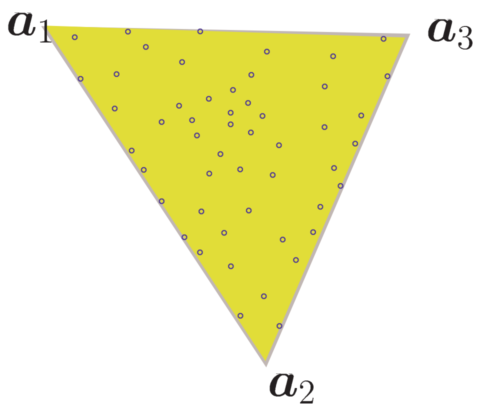

Simplex Volume Minimization: Intuition

Craig's belief [Craig1994]: the true endmembers may be located by finding a data enclosing simplex whose volume is the smallest.

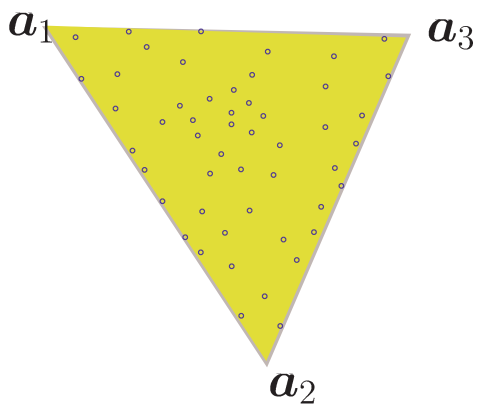

- **it seems volume min. (VolMin) can identify the true endmembers without pure pixels.**

Simplex Volume Minimization: Formulation

- **Formulation:**

$$
\begin{aligned}
\min_{\boldsymbol{a}_1,\ldots,\boldsymbol{a}_N \in \mathbb{R}^M} \quad & \mathrm{vol}(\boldsymbol{A}) \\
\text{s.t.} \quad & \boldsymbol{y}[n] \in \mathrm{conv}\{\boldsymbol{a}_1,\ldots,\boldsymbol{a}_N\}, \\
& n = 1,\ldots,L.
\end{aligned}
$$

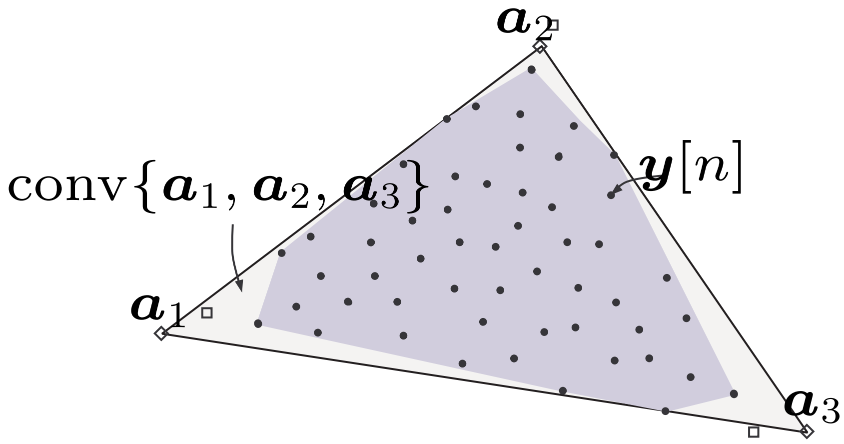

where

$$
\mathrm{vol}(\boldsymbol{A}) = \frac{1}{(N-1)!}\sqrt{\det(\bar{\boldsymbol{A}}^T\bar{\boldsymbol{A}})}, \quad \bar{\boldsymbol{A}} = [\ \boldsymbol{a}_1 - \boldsymbol{a}_N, \ldots, \boldsymbol{a}_{N-1} - \boldsymbol{a}_N\ ],
$$

- non-convex, NP-hard [Packer2008]

- algorithms rely on non-convex optimization

Simplex Volume Minimization: Optimization

- dimensionally reduce $\{\boldsymbol{y}[n]\}$ to $\{\boldsymbol{x}[n]\}$ such that $\boldsymbol{x}[n] = \boldsymbol{B}\boldsymbol{s}[n]$, $\boldsymbol{B} \in \mathbb{R}^{N-1 \times N}$.
- by transformation of a simplex to a polyhedron, recast VolMin as

$$\min_{\boldsymbol{B}} \ \mathrm{vol}(\boldsymbol{B}) \quad \text{s.t. } \boldsymbol{x}[n] \in \mathrm{conv}\{\boldsymbol{b}_1, \ldots, \boldsymbol{b}_N\}, \forall n \iff \max_{\boldsymbol{H},\boldsymbol{g}} |\det(\boldsymbol{H})| \quad \text{s.t. } \boldsymbol{H}\boldsymbol{x}[n] - \boldsymbol{g} \geq \boldsymbol{0}, \ (\boldsymbol{H}\boldsymbol{x}[n] - \boldsymbol{g})^T \boldsymbol{1} \leq 1, \forall n$$

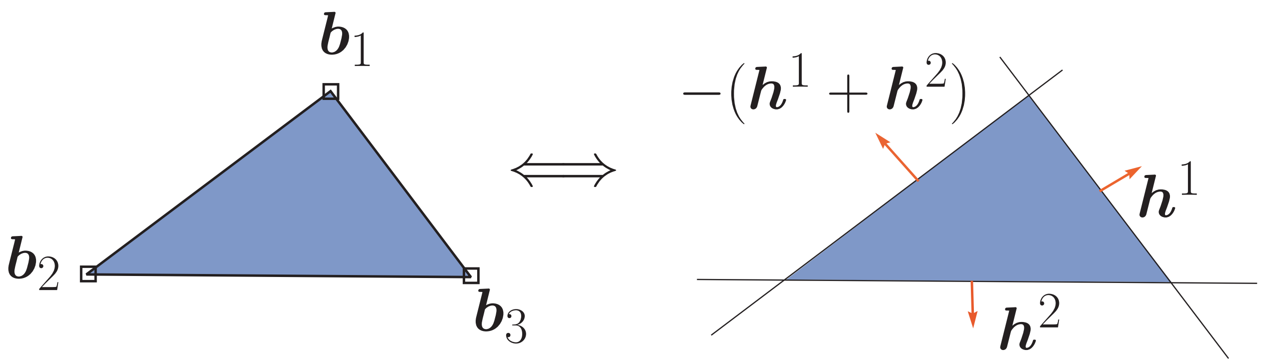

where $\boldsymbol{H} = [\boldsymbol{b}_1 - \boldsymbol{b}_N, \ldots, \boldsymbol{b}_{N-1} - \boldsymbol{b}_N]^{-1}$, $\boldsymbol{g} = \boldsymbol{H}\boldsymbol{b}_N$.

- algorithms: [Li-Bioucas2008], [Chan-Chi-Huang-Ma2009], [Bioucas2009]

Simplex Volume Minimization and Matrix Factorization

- recall the VolMin problem

$$\min_{\boldsymbol{a}_1,\ldots,\boldsymbol{a}_N} \mathrm{vol}(\boldsymbol{A}) \qquad \text{s.t. } \boldsymbol{y}[n] \in \mathrm{conv}\{\boldsymbol{a}_1,\ldots,\boldsymbol{a}_N\}, \quad n=1,\ldots,L$$

- by noting $\boldsymbol{y}[n] \in \mathrm{conv}\{\boldsymbol{a}_1,\ldots,\boldsymbol{a}_N\} \Longleftrightarrow \boldsymbol{y}[n] = \boldsymbol{A}\boldsymbol{s}_n$ for some $\boldsymbol{s}_n \geq \boldsymbol{0}, \boldsymbol{s}_n^T\boldsymbol{1} = 1$, VolMin can be equivalently written as

$$\min_{\boldsymbol{A},\boldsymbol{S}} \mathrm{vol}(\boldsymbol{A}) \qquad \text{s.t. } \boldsymbol{Y} = \boldsymbol{A}\boldsymbol{S},\ \boldsymbol{S} \geq \boldsymbol{0},\ \boldsymbol{S}^T\boldsymbol{1} = \boldsymbol{1}$$

- or, a regularized form may be considered:

$$\min_{\boldsymbol{A},\boldsymbol{S}\geq\boldsymbol{0},\boldsymbol{S}^T\boldsymbol{1}=\boldsymbol{1}} \|\boldsymbol{Y} - \boldsymbol{A}\boldsymbol{S}\|_F^2 + \lambda \cdot \mathrm{vol}(\boldsymbol{A}); \qquad \lambda > 0 \text{ is given,}$$

  which looks like a volume-regularized semi-NMF

  – do alternating opt. [Miao-Qi2007], [Fu-Huang-Yang-Ma-Sidiropoulos2016]

José Bioucas-Dias' Famous SISAL Scheme for VolMin

- consider the case of square $\boldsymbol{A}$, and consider the VolMin problem

$$\min_{\boldsymbol{A},\boldsymbol{S}} \log(|\det(\boldsymbol{A})|) \qquad \text{s.t. } \boldsymbol{Y} = \boldsymbol{A}\boldsymbol{S},\ \boldsymbol{S} \geq \boldsymbol{0},\ \boldsymbol{S}^T\boldsymbol{1} = \boldsymbol{1}$$

- by the change of variable $\boldsymbol{B} = \boldsymbol{A}^{-1}$, so that $\boldsymbol{S} = \boldsymbol{B}\boldsymbol{Y}$,

$$\min_{\boldsymbol{B}} -\log(|\det(\boldsymbol{B})|) \qquad \text{s.t. } \boldsymbol{B}\boldsymbol{Y} \geq \boldsymbol{0},\ \boldsymbol{Y}^T\boldsymbol{B}^T\boldsymbol{1} = \boldsymbol{1}$$

- SISAL [Bioucas2009]:

$$\min_{\boldsymbol{B}} -\log(|\det(\boldsymbol{B})|) + \lambda\rho(\boldsymbol{B}\boldsymbol{Y}) \qquad \text{s.t. } \boldsymbol{B}^T\boldsymbol{1} = (\boldsymbol{Y}^T)^\dagger\boldsymbol{1}$$

  where $\rho(\boldsymbol{X}) = \sum_{i,j} \max\{0, -x_{ij}\}$ is a penalty function for promoting non-negativity; $\lambda > 0$ is given.

- the problem is solved by a line-search-based proximal gradient method and ADMM

Numerical Demo.: Three Endmembers, Pure Pixel Case

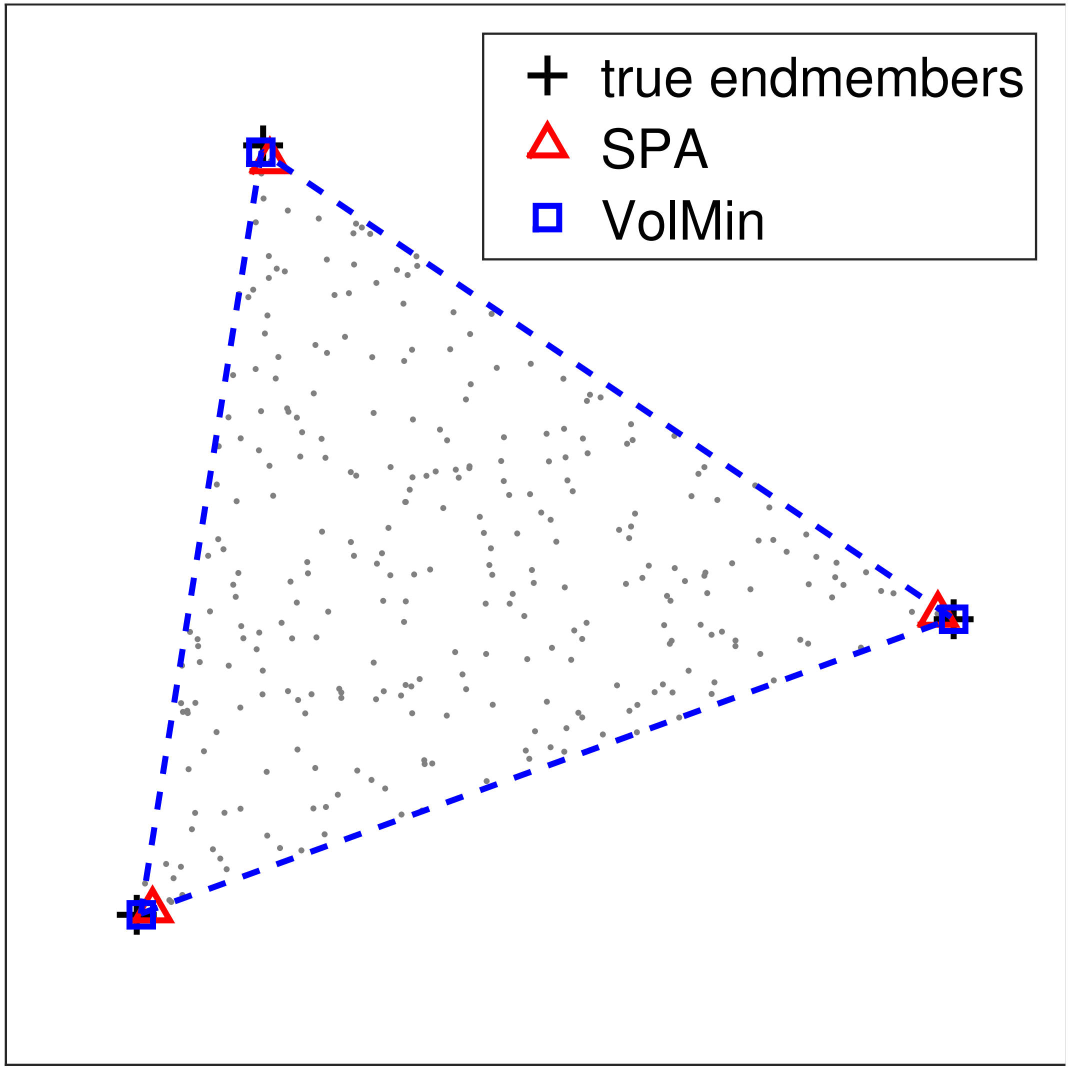

Numerical Demo.: Three Endmembers, No-Pure Pixel Case

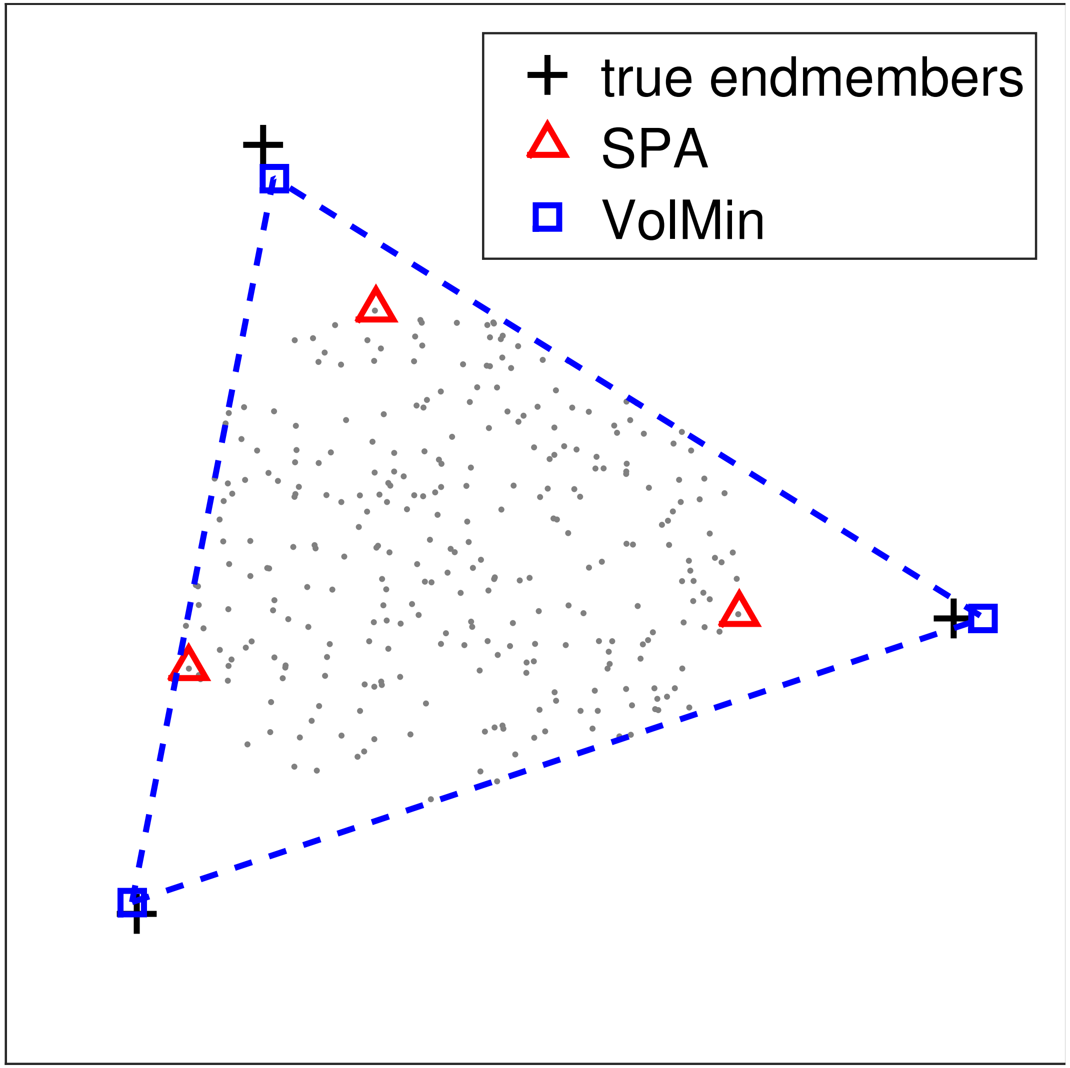

Numerical Demo.: Three Endmembers, No-Pure Pixel Case

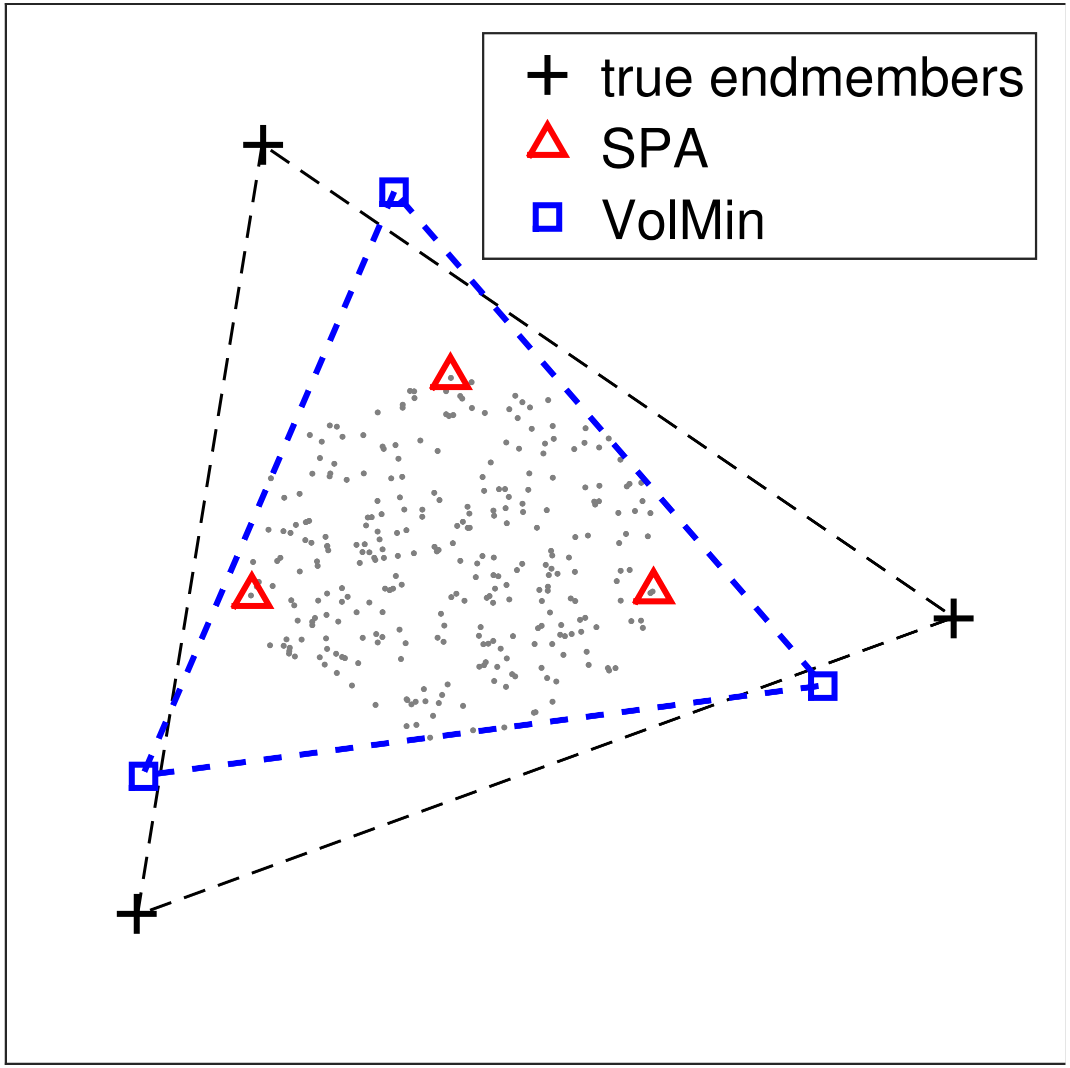

Simulation Results: Mean Squared Error Comparison

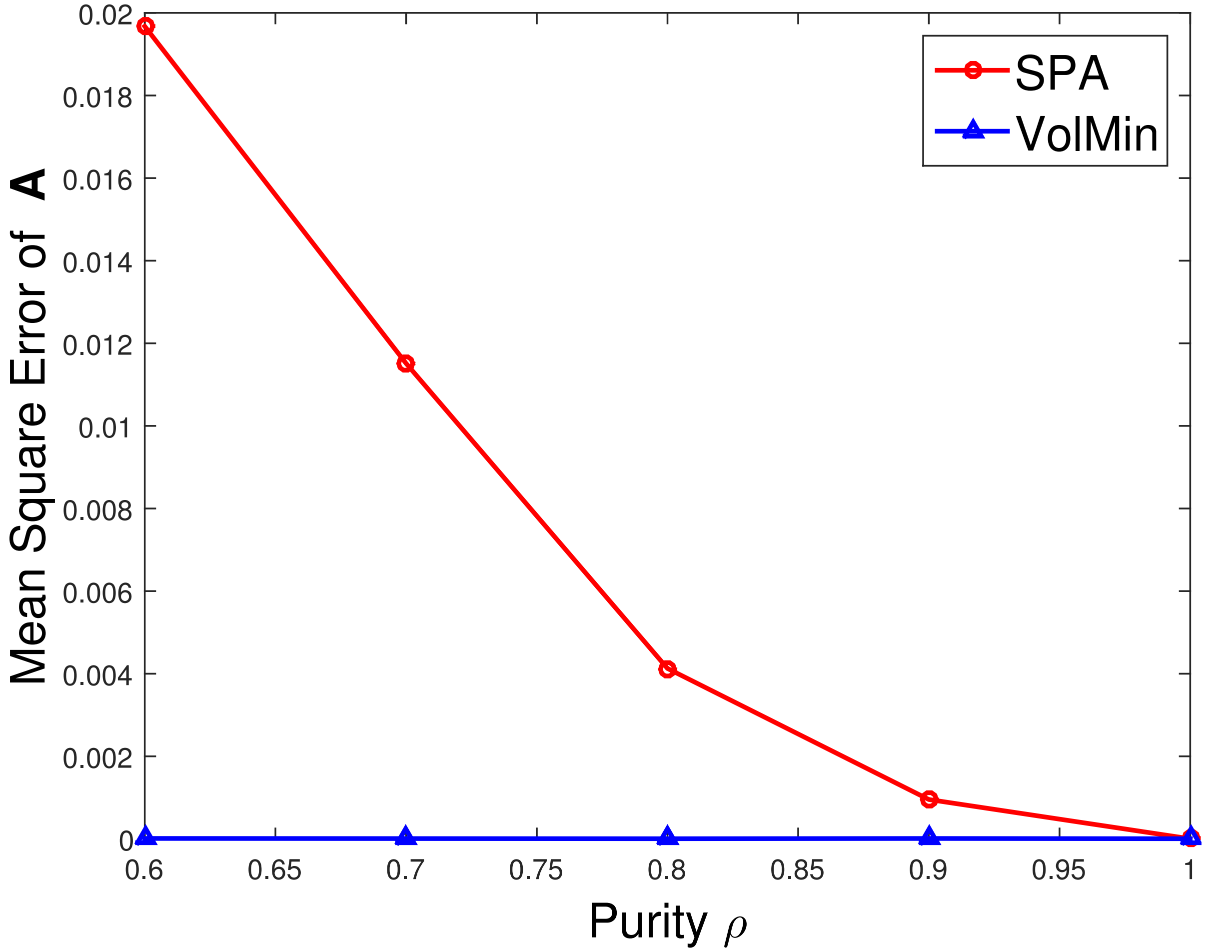

A Monte Carlo result. $N = 8$. "Purity ρ" describes the pixel purity: $\rho = 1$ corresponds to the pure pixel case, and $\rho = 1/\sqrt{N}$ the most heavily mixed case.

Unique Identifiability of VolMin

- numerical evidence suggests that VolMin works well without pure pixels
- **Question:** can we prove that VolMin can uniquely recover the true endmembers when the pure pixel assumption does not hold?
- **Answer: YES!** [Lin-Ma-Li-Chi-Ambikapathi2015], [Fu-Ma-Huang-Sidiropoulos2015]

Unique Identifiability of VolMin

Theorem [Lin-Ma-Li-Chi-Ambikapathi2015]: Suppose no noise, $N \geq 3$ and that $\boldsymbol{a}_1, \ldots, \boldsymbol{a}_N$ are linearly independent. Define

$$\gamma = \max \{ r \leq 1 \mid (\text{conv}\{\boldsymbol{e}_1, \ldots, \boldsymbol{e}_N\}) \cap \mathcal{B}(r) \subseteq \text{conv}\{\boldsymbol{s}_1, \ldots, \boldsymbol{s}_L\} \},$$

where $\mathcal{B}(r) = \{\boldsymbol{x} \mid \|\boldsymbol{x}\|_2 \leq r\}$. VolMin exactly recovers $\boldsymbol{a}_1, \ldots, \boldsymbol{a}_N$ if $\gamma > \frac{1}{\sqrt{N-1}}$.

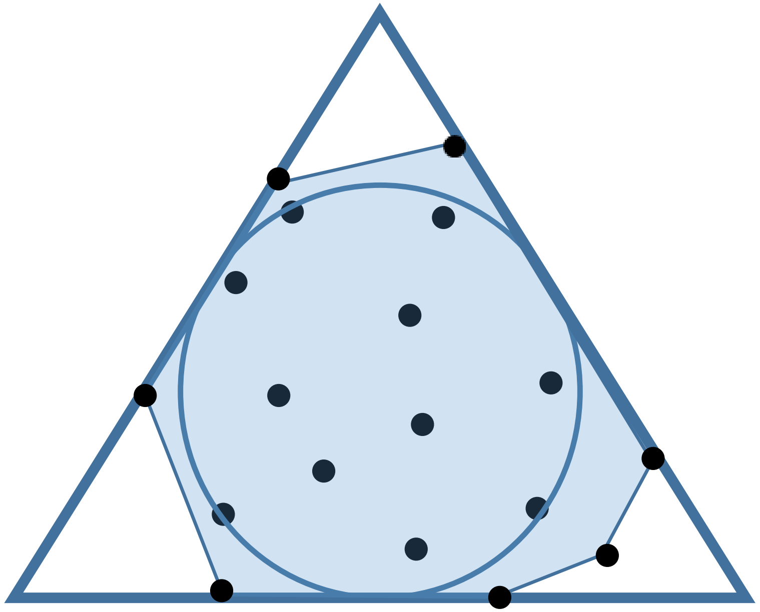

Unique Identifiability of VolMin

Theorem [Lin-Ma-Li-Chi-Ambikapathi2015]: Suppose no noise, $N \geq 3$ and that $\boldsymbol{a}_1, \ldots, \boldsymbol{a}_N$ are linearly independent. Define

$$\gamma = \max \{ r \leq 1 \mid (\mathrm{conv}\{\boldsymbol{e}_1, \ldots, \boldsymbol{e}_N\}) \cap \mathcal{B}(r) \subseteq \mathrm{conv}\{\boldsymbol{s}_1, \ldots, \boldsymbol{s}_L\}\}, \qquad (*)$$

where $\mathcal{B}(r) = \{\boldsymbol{x} \mid \|\boldsymbol{x}\|_2 \leq r\}$. VolMin exactly recovers $\boldsymbol{a}_1, \ldots, \boldsymbol{a}_N$ if $\gamma > \frac{1}{\sqrt{N-1}}$.

- much more relaxed than the pure pixel assumption (and separable NMF)
- arguably more relaxed than known NMF recovery conditions
  - [Donoho-Stodden2003]: require the pure pixel assumption
  - [Huang-Sidiropoulos-Swami2014]: require *both* $\boldsymbol{A}$ and $\boldsymbol{S}$ to satisfy $(*)$, roughly speaking, while VolMin requires *only* $\boldsymbol{S}$ to satisfy $(*)$
- [Fu-Huang-Sidiropoulos2018] further shows that VolMin can be applied to NMF without $\mathbf{1}^T \boldsymbol{s}[n] = 1$ and without column normalization preprocessing

Probabilistic Simplex Component Analysis (PRISM)

- VolMin assumes no noise, to begin with
- how about the noisy case?
- we consider statistical inference, which is a more disciplined approach to deal with noise

Probabilistic Simplex Component Analysis (PRISM)

- consider statistical inference akin to probabilistic PCA
- assume that $\boldsymbol{s}[n]$'s are i.i.d. distributed on the unit simplex
  - probabilistic PCA assumes i.i.d. Gaussian $\boldsymbol{s}[n]$'s
- in the noiseless case, the marginalized likelihood is

$$p_{\boldsymbol{A}}(\boldsymbol{y}[n]) = \int p_{\boldsymbol{A}}(\boldsymbol{y}[n]|\boldsymbol{s}[n])p(\boldsymbol{s}[n])d\boldsymbol{s}[n] = \frac{1}{\mathrm{vol}(\boldsymbol{A})}\mathbb{1}_{\mathcal{A}}(\boldsymbol{y}[n])$$

  where $\mathcal{A} = \mathrm{conv}\{\boldsymbol{a}_1, \ldots, \boldsymbol{a}_N\}$; $\mathbb{1}_{\mathcal{A}}(\boldsymbol{y}) = 1$ if $\boldsymbol{y} \in \mathcal{A}$, $\mathbb{1}_{\mathcal{A}}(\boldsymbol{y}) = 0$ if $\boldsymbol{y} \notin \mathcal{A}$

- maximum-likelihood estimator (alluded to in [Nascimento-Bioucas2012]):

$$\max_{\boldsymbol{A}} \sum_{n=1}^{L} \log(p_{\boldsymbol{A}}(\boldsymbol{y}[n])) = \max_{\boldsymbol{A}} -\log(\mathrm{vol}(\boldsymbol{A})) \text{ s.t. } \boldsymbol{y}[n] \in \mathcal{A}\ \forall n = \textbf{VolMin!}$$

- **Implication:** VolMin is PRISM when there is no noise

Probabilistic Simplex Component Analysis (PRISM)

- we study the noisy case [Wu-Ma-Li-So-Sidiropoulos2021]
- we show how volume-regularized factorization and SISAL are related to PRISM
- we show that, as the data length L goes to infinity, PRISM exactly identifies the true $\boldsymbol{A}$
- we consider variational inference as an algorithmic scheme for PRISM

Beyond HU:
Hyperspectral Super-Resolution

A Fundamental Limitation

- **Problem:** none of the known optical sensing systems can achieve both high spectral resolution and high spatial resolution

- hyperspectral cameras have high spectral resolution, but low spatial resolution

- RGB or multispectral cameras, on the other hand, can have high spatial resolution but low spectral resolution

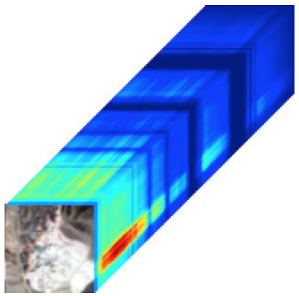

Hyperspectral Image

Multispectral Image

Hyperspectral Super-Resolution

- **Question:** can we have both high spectral and spatial resolution?

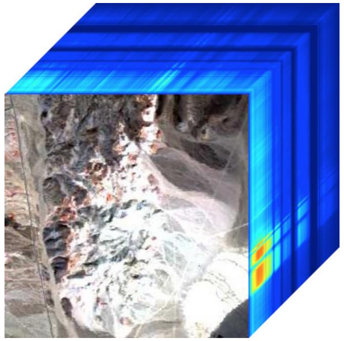

Super-resolution Image

- doing so has significant implications in many applications

Hyperspectral Super-Resolution

- **Question:** can we have both high spectral and spatial resolution?
- A Promising Candidate: fusion of a hyperspectral image and a multispectral image—a.k.a. hyperspectral super-resolution (HSR)

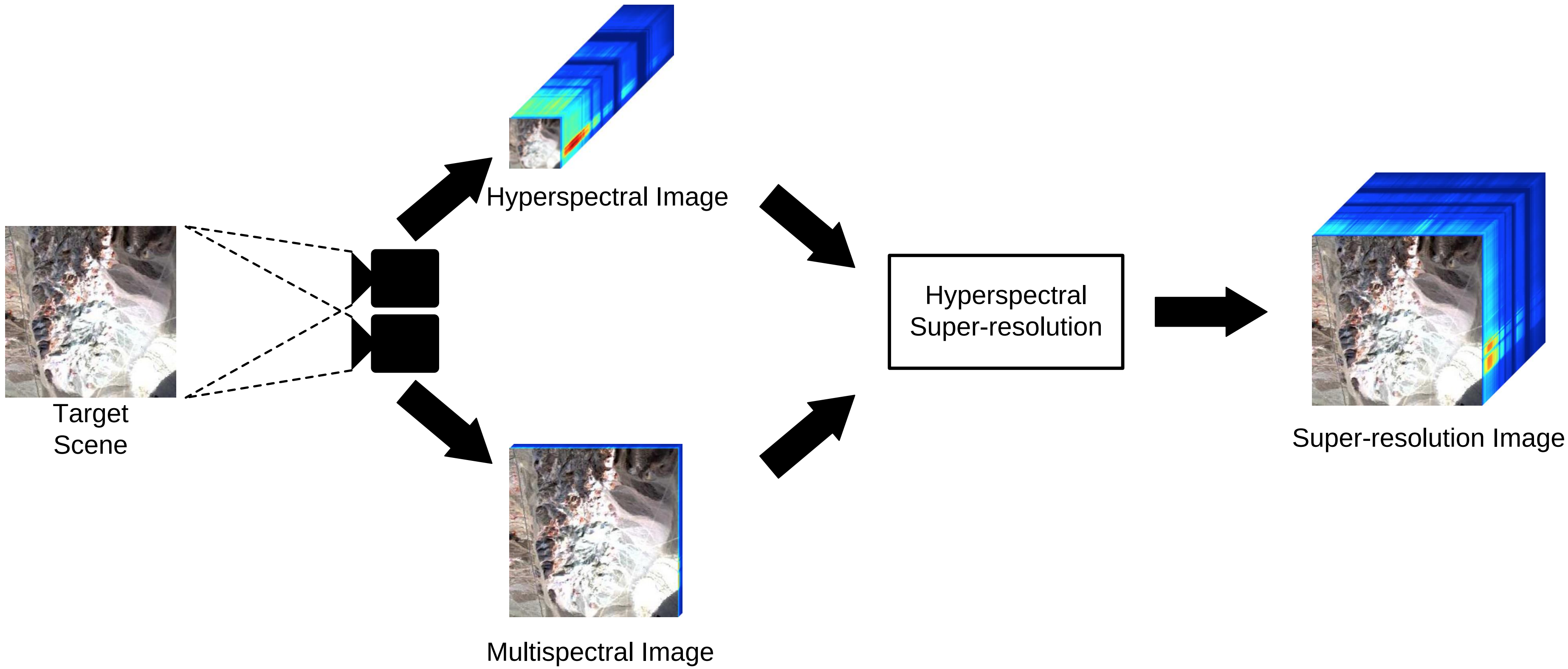

HSR Model

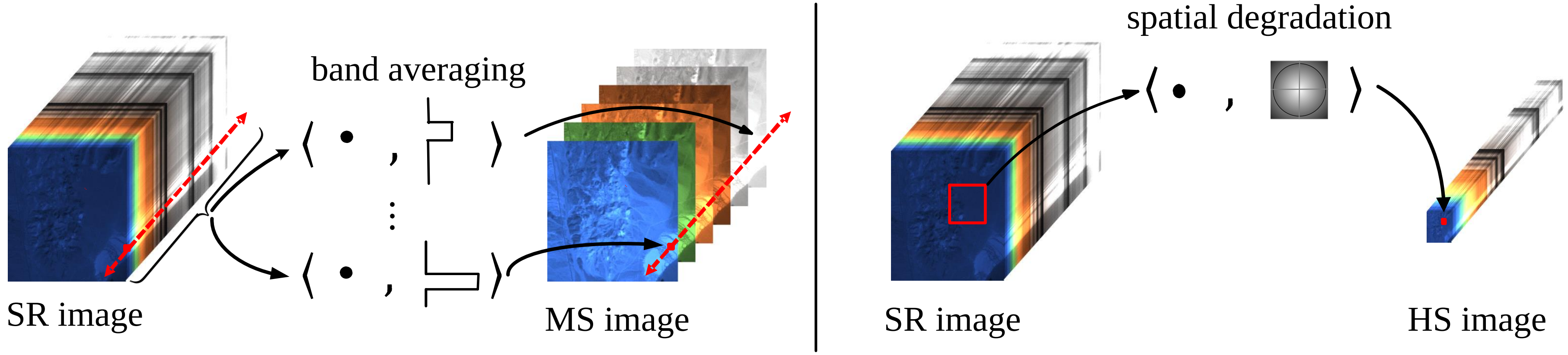

- **Model:** let $\boldsymbol{X}$ be the super-resolution image.

  hyperspectral image $= \boldsymbol{Y}_{\mathrm{H}} = \boldsymbol{X}\boldsymbol{G}$, $\quad \boldsymbol{G}$ being a (tall) spatial degradation matrix

  multispectral image $= \boldsymbol{Y}_{\mathrm{M}} = \boldsymbol{F}\boldsymbol{X}$, $\quad \boldsymbol{F}$ being a (fat) spectral degradation matrix

- **Issue:** the number of measurements (multispectral+hyperspectral) is much less than the number of the unknowns (the super-resolution image)

Hyperspectral Super-Resolution via Matrix Factorization

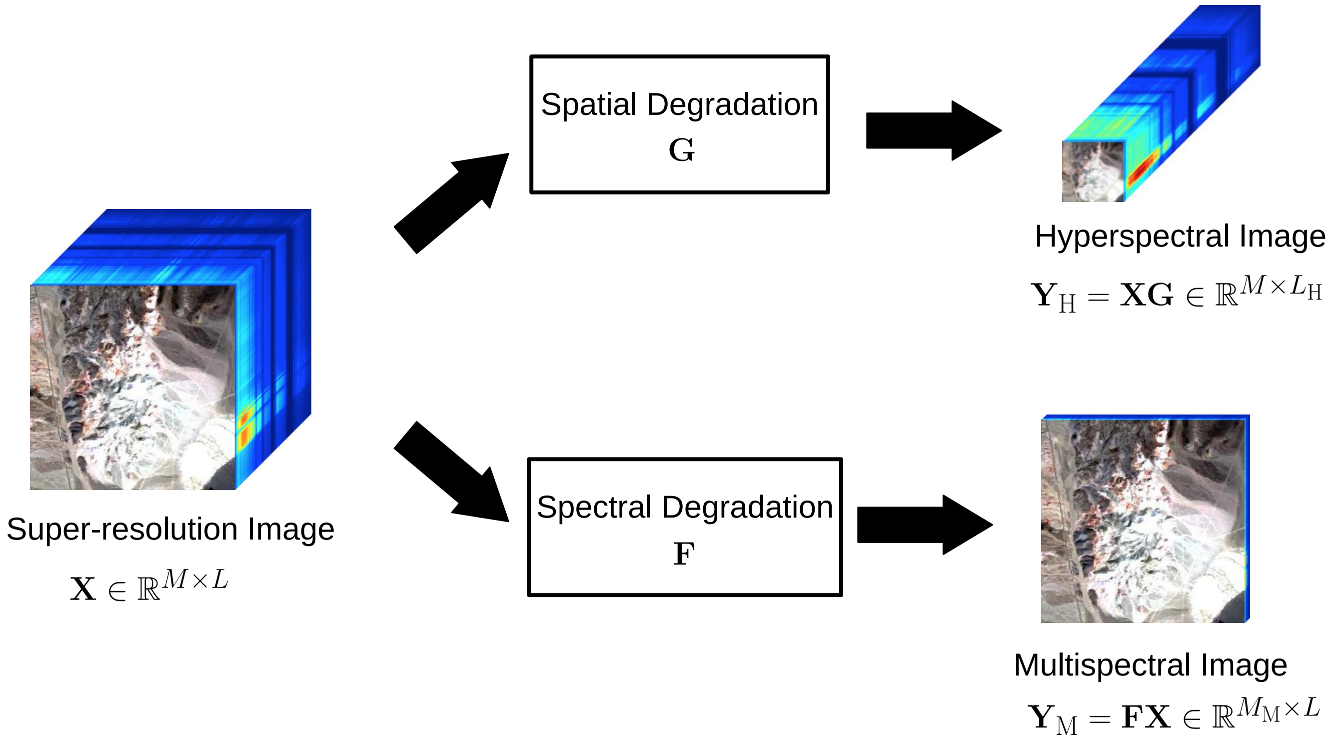

- **Idea:** use the HU model $\boldsymbol{X} = \boldsymbol{AS}$, and solve

$$\min_{\boldsymbol{A},\boldsymbol{S}} \|\boldsymbol{Y}_{\rm H} - \boldsymbol{ASG}\|_F^2 + \|\boldsymbol{Y}_{\rm M} - \boldsymbol{FAS}\|_F^2 \quad \text{s.t. appropriate constraints on } \boldsymbol{A}, \boldsymbol{S}$$

- reminiscent of matrix completion

Hyperspectral Super-Resolution via Matrix Factorization

- first proposed in [Kawakmai-Matsushita-*et al.*'11] for computer vision and in [Yokoya-Yairi-Iwaski'12] for remote sensing

- received much attention, has many algorithms these days

- our interest: algorithmic schemes that have identifiability guarantees; see [Li-Ma-Wu-Liu2023] and the references therein

Separable Coupled Factorization (SECO) for HSR

- we don't want to solve the coupled factorization

$$\min_{\boldsymbol{A},\boldsymbol{S}} \|\boldsymbol{Y}_{\rm H} - \boldsymbol{ASG}\|_F^2 + \|\boldsymbol{Y}_{\rm M} - \boldsymbol{FAS}\|_F^2 \quad \text{s.t. appropriate constraints on } \boldsymbol{A}, \boldsymbol{S}$$

- let $\boldsymbol{C} = \boldsymbol{SG}$, and note $\boldsymbol{Y}_{\rm H} = \boldsymbol{AC}$.

- SECO Step 1: retrieve $\boldsymbol{A}$ from $\boldsymbol{Y}_{\rm H}$ by pure pixel search (or VolMin)
  - idea: solve a structured factorization problem $\min_{\boldsymbol{A},\boldsymbol{C}} \|\boldsymbol{Y}_{\rm H} - \boldsymbol{AC}\|_F^2$ first

- SECO Step 2: given the retrieved $\boldsymbol{A}$ in Step 1, retrieve $\boldsymbol{S}$ from $\boldsymbol{Y}_{\rm M}$ by

$$\min_{\boldsymbol{S}} \|\boldsymbol{Y}_{\rm M} - \boldsymbol{FAS}\|_F^2$$

- we show that, if $\boldsymbol{S}$ satisfies some sparsity and pure-pixel assumptions, then, with a certain modification of Step 2, we can exactly recover $\boldsymbol{A}$ and $\boldsymbol{S}$ [Li-Ma-Wu-Liu2023]

A Semi-Real Experiment Result for HSR

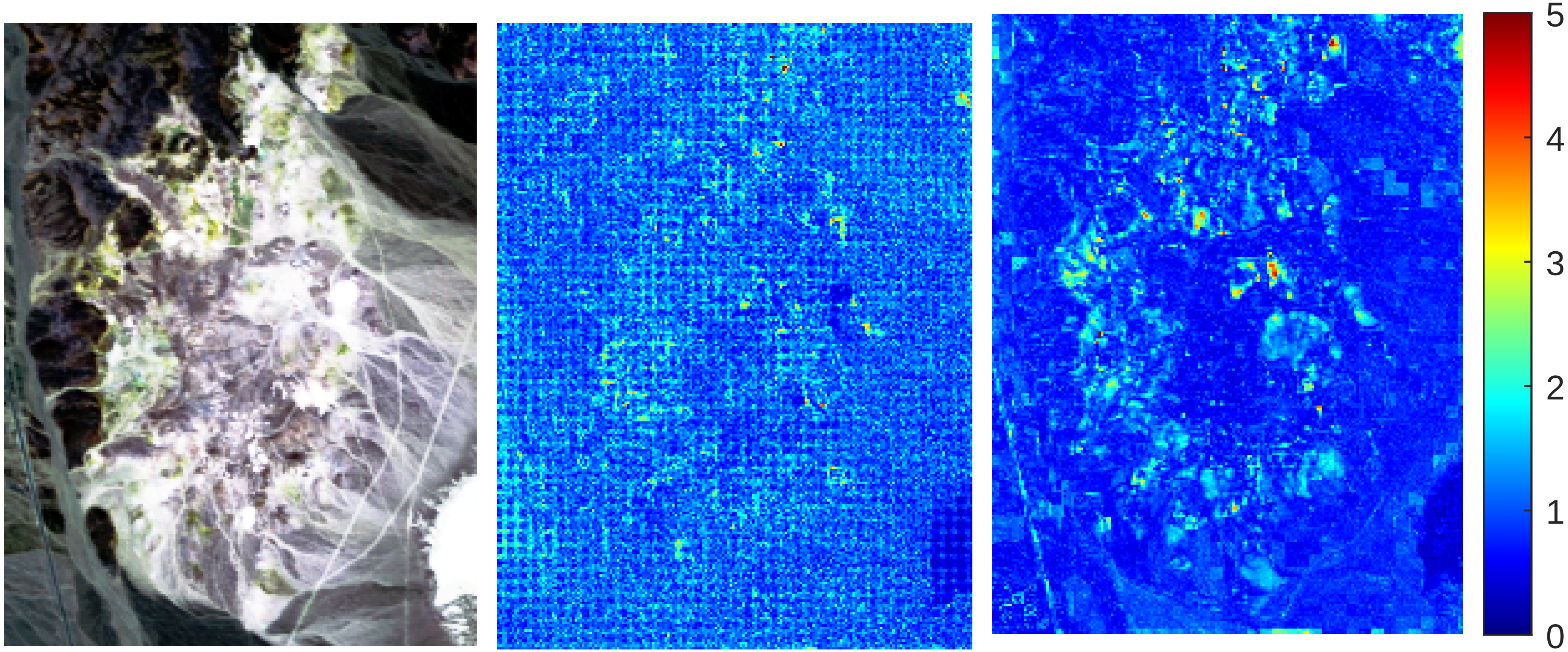

Left: The color composite image of the super-resolution image.
Middle: spectral angle mapper (SAM) of coupled factorization. Mean SAM $= 1.15$, runtime $= 88.09$ seconds.
Right: SAM of SECO. Mean SAM $= 0.89$, runtime$= 2.57$ seconds.

Conclusion and Discussion

- what are the great insights to learn from HU in remote sensing?
  - convex geometry, pure pixel search, volume minimization
- other than hyperspectral imaging, what is worthwhile to note?
  - its connections to important problems in machine learning and data science

Thank You! Main References of This Talk

W.-K. Ma, J. M. Bioucas-Dias, T.-H. Chan, N. Gillis, *et al.*, "A signal processing perspective on hyperpsectral unmixing," *IEEE SP Mag.*, Jan. 2014.

N. Gillis, "The why and how of nonnegative matrix factorization," in *Regularization, Optimization, Kernels, and Support Vector Machines*, 2014.

X. Fu, K. Huang, N. D. Sidiropoulos, and W.-K. Ma, "Nonnegative matrix factorization for signal and data analytics: Identifiability, algorithms, and applications," *IEEE SP Mag.*, 2019.

References

Pure Pixel Search:

[Boardman-Kruse-Green1995] J. Boardman, F. Kruse, and R. Green, "Mapping target signatures via partial unmixing of AVIRIS data," in *Proc. Summ. JPL Airborne Earth Sci. Workshop*, vol. 1, Pasadena, CA, Dec. 1995, pp. 23–26.

[Nascimento-Bioucas2003] J. Nascimento and J. M. Bioucas-Dias, "Vertex component analysis: A fast algorithm to extract endmembers spectra from hyperspectral data," in *Pattern Recognition and Image Analysis: 1st Iberian Conf.*, 2003, pp. 626–635.

[Chan-Ma-Ambikapathi-Chi2011] T.-H. Chan, W.-K. Ma, A. Ambikapathi, and C.-Y. Chi, "A simplex volume maximization framework for hyperspectral endmember extraction," *IEEE Trans. Geosci. Remote Sens.*, vol. 49, no. 11, pp. 4177–4193, 2011.

[Gillis-Vavasis2014] N. Gillis and S. Vavasis, "Fast and robust recursive algorithms for separable nonnegative matrix factorization," *IEEE Trans. Pattern Anal. Mach. Intell.*, vol. 36, no. 4, pp. 698–714, April 2014.

[Fu-Ma-Chan-Bioucas2015] X. Fu, W.-K. Ma, T.-H. Chan, and J. M. Bioucas-Dias, "Self-dictionary sparse regression for hyper spectral unmixing: Greedy pursuit and pure pixel search are related," *J. Select. Topics Signal Process.*, Sep. 2015.

[Elhamifar-Sapiro-Vidal2012] E. Elhamifar, G. Sapiro, and R. Vidal, "See all by looking at a few: Sparse modeling for finding representative objects," in *Proc. IEEE CVPR 2012*, 2012, pp. 1600–1607.

[Arora-Ge-Kannan-Moitra2012] S. Arora, R. Ge, R. Kannan, and A. Moitra, "Computing a nonnegative matrix factorization—Provably," in *Proc. 44th Symp. Theory of Computing*, ACM, 2012, pp. 145–162.

[Recht-Re-Tropp-Bittorf2012] B. Recht, C. Re, J. Tropp, and V. Bittorf, "Factoring nonnegative matrices with linear programs," in *Advances in Neural Information Processing Systems*, 2012, pp. 1214–1222.

[Esser-Moller-Osher-Sapiro-Xin2012] E. Esser, M. Moller, S. Osher, G. Sapiro, and J. Xin, "A convex model for nonnegative matrix factorization and dimensionality reduction on physical space," *IEEE Trans. Image Process.*, vol. 21, no. 7, pp. 3239–3252, Jul. 2012.

History of Convex Geometry and Applications:

[Craig1990] M. D. Craig, "Unsupervised unmixing of remotely sensed images," in *Proc. Australasian Remote Sens. Conf.*, Perth, Australia, 1990, pp. 324–330.

[Craig1994] M. D. Craig, "Minimum-volume transforms for remotely sensed data," *IEEE Trans. Geosci. Remote Sens.*, vol. 32, no. 3, pp. 542–552, May 1994.

[Boardman-Kruse-Green1995] J. Boardman, F. Kruse, and R. Green, "Mapping target signatures via partial unmixing of AVIRIS data," in *Proc. Summ. JPL Airborne Earth Sci. Workshop*, vol. 1, Pasadena, CA, Dec. 1995, pp. 23–26.

[Winter1999] M. E. Winter, "N-FINDR: An algorithm for fast autonomous spectral end- member determination in hyperspectral data," in *Proc. SPIE Conf. Imaging Spectrometry*, Pasadena, CA, Oct. 1999, pp. 266–275.

[Imbrie1964] J. Imbrie, "Vector analysis of heavy-mineral data," *Geological Society of America Bulletin*, vol. 75, pp. 1131–1156, Nov. 1964.

[Full-Ehrlich-Klovan1981] W. E. Full, R. Ehrlich, and J. E. Klovan, "EXTENDED QMODEL—objective definition of external endmembers in the analysis of mixtures," *Mathematical Geology*, vol. 13, no. 4, pp. 331–344, 1981.

[Perczel et al. 1989] A. Perczel, M. Hollosi, G. Tusnady, and D. Fasman, "Convex constraint decomposition of circular dichroism curves of proteins,"' *Croatica Chim. Acta*, vol. 62, pp. 189–200, 1989.

[Naanaa-Nuzillard2005] "Blind source separation of positive and partially correlated data," *Signal Processing*, vol. 85, no. 9, pp. 1711–1722, 2005.

[Chan-Ma-Chi-Wang2008] T.-H. Chan, W.-K. Ma, C.-Y. Chi, & Y. Wang, "A convex analysis framework for blind separation of non-negative sources," *IEEE Trans. Signal Process.*, vol. 56, no. 10, pp. 5120–5134, 2008.

[Fu-Ma-Huang-Sidiropoulos2015] X. Fu, W.-K. Ma, K. Huang, and N. D. Sidiropoulos, "Blind separation of quasi-stationary sources: Exploiting convex geometry in covariance domain," *IEEE Trans. Signal Process.*, 2015.

Simplex Volume Minimization:

[Craig1994] M. D. Craig, "Minimum-volume transforms for remotely sensed data," *IEEE Trans. Geosci. Remote Sens.*, vol. 32, no. 3, pp. 542–552, May 1994.

[Packer2008] A. Packer, "NP-hardness of largest contained and smallest containing simplices for V- and H-polytopes," Discrete and Computational Geometry, vol. 28, no. 3, pp. 349–377, 2002.

[Li-Bioucas2008] J. Li and J. Bioucas-Dias, "Minimum volume simplex analysis: A fast algorithm to unmix hyperspectral data," in *Proc. IEEE IGARSS*, Aug. 2008, pp. 250–253.

[Chan-Chi-Huang-Ma2009] T.-H. Chan, C.-Y. Chi, Y.-M. Huang, and W.-K. Ma, "A convex analysis-based minimum-volume enclosing simplex algorithm for hyperspectral unmixing," *IEEE Trans. Signal Process.,* 2009.

[Bioucas2009] J. M. Bioucas-Dias, "A variable splitting augmented Lagrangian approach to linear spectral unmixing," in *Proc. IEEE WHISPERS*, Aug. 2009.

[Miao-Qi2007] L. Miao and H. Qi, “Endmember extraction from highly mixed data using minimum volume constrained nonnegative matrix factorization,” *IEEE Trans. Geosci. Remote Sens.*, 2007.

[Fu-Huang-Yang-Ma-Sidiropoulos2016] X. Fu, K. Huang, B. Yang, W.-K. Ma, and N. D. Sidiropoulos, “Robust volume minimization-based matrix factorization for remote sensing and document clustering,” *IEEE Trans. Signal Process.*, 2016.

[Lin-Ma-Li-Chi-Ambikapathi2015] C.-H. Lin, W.-K. Ma, W.-C. Li, C.-Y. Chi, and A. Ambikapathi, “Identifiability of the simplex volume minimization criterion for blind hyperspectral unmixing: The no pure-pixel case,” *IEEE Trans. Geosci. Remote Sens.*, Oct. 2015.

[Fu-Huang-Sidiropoulos2018] X. Fu, K. Huang, and N. D. Sidiropoulos, “On identifiability of nonnegative matrix factorization,” *IEEE Signal Process. Lett.*, 2018.

[Nascimento-Bioucas2012] J. Nascimento and J. Bioucas, “”Hyperspectral unmixing based on mixtures of Dirichlet components,” *IEEE Trans. Geosci. Remote Sens.*, 2012.

Others:

[Donoho-Stodden2003] D. Donoho and V. Stodden, “When does non-negative matrix factorization give a correct decomposition into parts?” in *Advances in Neural Information Processing Systems*, 2003, pp. 1141–1148.

[Huang-Sidiropoulos-Swami2014] K. Huang, N. D. Sidiropoulos and A. Swami, "Non-negative matrix factorization revisited: Uniqueness and algorithm for symmetric decomposition," *IEEE Trans. Signal Process.*, vol. 62, no. 1, pp. 211–224, 2014.

[Wu-Ma-Li-So-Sidiropoulos2021] R. Wu, W.-K. Ma, Y. Li, A.-M.-C. So, and N. D. Sidiropoulos, "Probabilistic simplex component analysis," *IEEE Trans. Signal Process.*, 2021.

[Li-Ma-Wu-Liu2023] Y. Li, W.-K. Ma, R. Wu, and H. Liu, "A simple scheme for coupled factorization for hyperspectral super-resolution: Exploiting sparsity in an easy way," in *2023 ICASSP*.